Vaccination with *Plasmodium vivax* Duffy-binding protein inhibits parasite growth during controlled human malaria infection

Mimi M. Hou[1,2,3], Jordan R. Barrett[1,2,3], Yrene Themistocleous[2], Thomas A. Rawlinson[2], Ababacar Diouf[4], Francisco J. Martinez[5], Carolyn M. Nielsen[1,2,3], Amelia M. Lias[1,2,3], Lloyd D. W. King[1,2,3], Nick J. Edwards[2], Nicola M. Greenwood[2], Lucy Kingham[2], Ian D. Poulton[2], Baktash Khozoee[2], Cyndi Goh[2], Susanne H. Hodgson[1,2,3], Dylan J. Mac Lochlainn[1,2,3], Jo Salkeld[1,2,3], Micheline Guillotte-Blisnick[5], Christèle Huon[5], Franziska Mohring[6], Jenny M. Reimer[7], Virander S. Chauhan[8], Paushali Mukherjee[9], Sumi Biswas[2], Iona J. Taylor[2], Alison M. Lawrie[2], Jee-Sun Cho[1,2,3], Fay L. Nugent[2], Carole A. Long[4], Robert W. Moon[6], Kazutoyo Miura[4], Sarah E. Silk[1,2,3], Chetan E. Chitnis[5], Angela M. Minassian[1,2,3,10,*], and Simon J. Draper[1,2,3,10,*].

Affiliations:

[1] Department of Biochemistry, University of Oxford; Oxford, OX1 3QU, UK.

[2] The Jenner Institute, University of Oxford; Oxford, OX3 7DQ, UK.

[3] Kavli Institute for Nanoscience Discovery, University of Oxford, Oxford, OX1 3QU, UK.

[4] Laboratory of Malaria and Vector Research, NIAID/NIH; Rockville, MD 20852, USA.

[5] Unité de Biologie de Plasmodium et Vaccins, Institut Pasteur, Université Paris Cité; 25-28 Rue du Dr Roux, 75015 Paris, France.

[6] Department of Infection Biology, London School of Hygiene and Tropical Medicine; London, WC1E 7HT, UK.

[7] Novavax AB; Kungsgatan 109, SE-753 18, Uppsala, Sweden.

[8] International Centre for Genetic Engineering and Biotechnology (ICGEB); New Delhi, India.

[9] Multi-Vaccines Development Program (MVDP); New Delhi, India.

[10] NIHR Oxford Biomedical Research Centre, Oxford, UK.

* These authors contributed equally.

Correspondence to: chetan.chitnis@pasteur.fr, angela.minassian@bioch.ox.ac.uk, simon.draper@bioch.ox.ac.uk

This manuscript has been accepted for publication in Science Translational Medicine. This version has not undergone final editing. Please refer to the complete version of record at www.sciencetranslationalmedicine.org/. The manuscript may not be reproduced or used in any manner that does not fall within the fair use provisions of the Copyright Act without the prior written permission of AAAS.

Abstract

There are no licensed vaccines against *Plasmodium vivax*. We conducted two Phase I/IIa clinical trials to assess two vaccines targeting *P. vivax* Duffy-binding protein region II (PvDBPII). Recombinant viral vaccines using chimpanzee adenovirus 63 (ChAd63) and modified vaccinia virus Ankara (MVA) vectors, as well as a protein and adjuvant formulation (PvDBPII/Matrix-M) were tested in both a standard and delayed dosing regimen. Volunteers underwent controlled human malaria infection (CHMI) following their last vaccination, alongside unvaccinated controls. Efficacy was assessed by comparison of parasite multiplication rate in blood. PvDBPII/Matrix-M, given in a delayed dosing regimen, elicited the highest antibody responses and reduced the mean parasite multiplication rate following CHMI by 51% (n=6) compared to unvaccinated controls (n=13), whereas no other vaccine or regimen impacted parasite growth. Both viral-vectored and protein vaccines were well tolerated and elicited expected, short lived adverse events. Together, these results support further clinical evaluation of the PvDBPII/Matrix-M *P. vivax* vaccine.

One-Sentence Summary: The PvDBPII/Matrix-M vaccine, which targets the *Plasmodium vivax* Duffy-binding protein, reduced growth of malaria parasites in blood of humans.

Introduction

Plasmodium vivax is the second most common cause of malaria and most geographically widespread, causing an estimated 4.5 million cases in 2020 (*1*). Control of *P. vivax* is more challenging than *P. falciparum* due to several factors. These include the ability of *P. vivax* to form dormant liver-stage hypnozoites that can reactivate and lead to relapsing blood-stage parasitemia, and earlier production of gametocytes in the blood-stage resulting in more rapid transmission (*2*). An effective vaccine would greatly aid elimination efforts worldwide but few *P. vivax* vaccines have reached clinical development.

Candidate vaccines against *P. vivax* have been developed that target different stages of the parasite's lifecycle (*3*). These include blood-stage vaccines that aim to inhibit the invasion of reticulocytes by merozoites, the stage of infection causing clinical disease. The leading blood-stage vaccine target is *P. vivax* Duffy-binding protein (PvDBP), which binds to the Duffy antigen receptor for chemokines (DARC/Fy) on reticulocytes to mediate invasion of the parasite (*4*). This interaction is critical as evidenced by the natural resistance of Duffy antigen negative individuals to *P. vivax* malaria (*5*). However, the efficacy of blocking this molecular interaction with vaccine-induced antibodies has not been tested previously in clinical trials.

Two vaccines targeting region II of PvDBP (PvDBPII), a 327-amino acid domain that binds to DARC, have previously progressed to Phase I clinical trials. These vaccines comprise a recombinant viral-vectored chimpanzee adenovirus 63 (ChAd63)-modified vaccinia virus Ankara (MVA) platform (*6*) and a protein/adjuvant formulation (PvDBPII/GLA-SE) (*7*). Both vaccines encode the Salvador I (SalI) allele of PvDBPII and were shown to induce binding-inhibitory antibodies (BIA) that block the interaction of recombinant PvDBPII to the DARC receptor in vitro (*6, 7*).

Here we report results from two Phase I/IIa clinical trials in healthy malaria-naïve adults using either the same viral-vectored vaccine or the PvDBPII protein vaccine reformulated in Matrix-M adjuvant. Both vaccines were tested for efficacy for the first time by blood-stage controlled human malaria infection (CHMI) using the heterologous PvW1 clone of *P. vivax* (*8*).

Results

Participants and trial design

Sixteen volunteers were enrolled into the VAC071 trial testing the viral-vectored vaccines (VV-PvDBPII) between July 2019 and July 2021 (**Fig. 1A**). Three volunteers in Group 1 received ChAd63 followed by MVA PvDBPII at 0 and 2 months. Ten volunteers in Group 2 received ChAd63 PvDBPII in February 2020, prior to the trial being halted due to the coronavirus disease 2019 (COVID-19) pandemic. After restart of the trial, two of the ten volunteers were re-enrolled and received a second dose of ChAd63 PvDBPII at 17 months, followed by MVA PvDBPII at 19 months. Three volunteers enrolled into Group 3 received one dose of ChAd63 followed by MVA PvDBPII at 0 and 2 months. Vaccinees underwent CHMI 2 to 4 weeks after their final vaccination.

Sixteen volunteers were enrolled into the VAC079 trial testing the protein vaccine PvDBPII in Matrix-M adjuvant (PvDBPII/M-M) between January 2020 and July 2021 (**Fig. 1B**). Twelve volunteers enrolled into Group 1 in 2020 received two doses of PvDBPII/M-M at 0 and 1 months before the trial was halted due to the COVID-19 pandemic. After restart of the trial in 2021, eight of the twelve volunteers were re-enrolled and received a third vaccination at 14 months and six of these volunteers underwent CHMI 2 to 4 weeks later. Four volunteers enrolled into Group 2 in July 2021 received three doses of PvDBPII/M-M at 0, 1 and 2 months, followed by CHMI 2 to 4 weeks later.

Thirteen infectivity control volunteers underwent CHMI in parallel with vaccinees over three phases of the VAC069 study (**Fig. 1C and D**). Demographics of volunteers in each trial are provided in **table**

S1. Control volunteers were followed-up to 3 months post-CHMI. Vaccinees were followed-up to 9 months post-CHMI, apart from i) the final study visits for Group 1 volunteers in VAC071 fell during the trial halt and were conducted remotely by telephone without phlebotomy; and ii) five out of six Group 1 volunteers from the VAC079 trial who completed CHMI were enrolled into a new study group at 3 months post-CHMI and their data after this timepoint are not reported here.

Vaccine safety

No safety concerns were identified with the viral-vectored or protein-in-adjuvant vaccines and no serious adverse events (AE) occurred in the VAC071 and VAC079 trials. The viral-vectored vaccines showed similar reactogenicity to that previously reported (*6*). Solicited AEs were predominantly mild to moderate in severity, with pain at the injection site and fatigue being most common (**Fig. 2A and B**). Three severe solicited AEs occurred post-vaccination, all of which resolved within 48 hours: nausea in one individual following ChAd63 PvDBPII vaccination, and feverishness and pyrexia in another individual following MVA PvDBPII vaccination. Solicited AEs following vaccinations with PvDBPII/M-M were all mild to moderate in severity and no severe adverse events occurred (**Fig. 2C**). Injection site pain and headache were the most common solicited AEs. Transient lymphopenia, with maximal severity of grade 2, occurred commonly following vaccinations with both the viral-vectored and protein-in-adjuvant vaccines (**table S2**). Unsolicited AEs deemed at least possibly related to either viral-vectored or protein-in-adjuvant vaccinations were of mild to moderate severity and self-limited (**tables S3 and S4**).

Viral-vectored and protein PvDBPII vaccines elicited antibody responses.

Anti-PvDBPII (SalI) total IgG serum antibody responses peaked around 2 weeks following the final vaccination in all regimens (**Fig. 3A**). PvDBPII/M-M given at 0, 1, and 14 months induced the highest antibody response at this timepoint (geometric mean 198 μg/mL [range 153 to 335]), which was significantly higher than the viral-vectored vaccines (29 μg/mL [range 9 to 85]; $p<0.001$) (**Fig. 3B**). Anti-PvDBPII antibody responses were negative (less than 1 μg/mL) in all vaccinees prior to their first vaccination, and in controls remained below 1 μg/mL throughout. Antibody responses waned

relatively quickly from their peak during the first month, with no boosting observed during CHMI, followed by a slower rate of decline which plateaued in some volunteers by 10 months post-final vaccination. Antibody longevity for each individual was estimated by calculating the area under the curve (AUC) from the time of the peak antibody concentration to the final timepoint available, divided by the peak antibody concentration and duration over which the AUC was calculated. Antibody longevity did not differ between different dosing regimens (**fig. S1**).

PvDBPII-specific $CD4^+$ $CD45RA^-$ $CCR7^-$ effector memory T cells producing interferon (IFN)-γ were detectable following final vaccinations with VV-PvDBPII and PvDBPII/M-M administered in a delayed dosing regimen (**Fig. 3C**). IFN-γ producing $CD8^+$ effector memory T cells were observed at low frequencies in the VV-PvDBPII vaccinees and were not detectable in the protein vaccine groups (**fig. S2** and **S3, table S5**).

Serum taken pre-CHMI from vaccinees administered PvDBPII/M-M in the delayed dosing regimen showed roughly 10-fold higher BIA values (geometric mean of dilution factor to achieve 50% binding inhibition (IC_{50}) = 1224 [range 643 to 3026]) as compared to the monthly dosing regimen and VV-PvDBPII (**Fig. 3D**). Using the dilution factor and total IgG concentration in the serum, the concentration of anti-PvDBPII total IgG that is required to achieve 50% binding inhibition was calculated for each individual. This was lower in the PvDBPII/M-M delayed dosing regimen group (median 123 ng/mL [range 78 to 250]) as compared to the monthly regimen of PvDBPII/M-M (447 ng/mL [196-715]; p=0.05) (**fig. S4**). The binding inhibition IC_{50} in the VV-PvDBPII group did not differ from the other groups when all 8 vaccinees' data were combined but the two vaccinees who received a second dose of ChAd63 PvDBPII after the trial halt had a low binding inhibition IC_{50} of 62 and 140 ng/mL.

158 Functional anti-parasitic in vitro growth inhibition activity (GIA) was generally low pre-CHMI. The
159 highest activity was observed in the PvDBPII/M-M delayed dosing regimen with median GIA of 29%
160 (range 7 to 45%) against transgenic *P. knowlesi* expressing the PvDBP PvW1 allele (challenge
161 sequence) (**Fig. 3E**). GIA against *P. knowlesi* expressing the PvDBP SalI allele (vaccine sequence)
162 were similar and correlated well with GIA against the PvW1 allele (**fig. S5A and B**). Serum IgG
163 responses and BIA assayed using the PvW1 sequence of PvDBPII were also well correlated and in
164 concordance with responses to the SalI PvDBPII sequence (**Fig. S5C to E**). BIA correlated strongly
165 with anti-PvDBPII total IgG serum antibody responses measured by ELISA, whilst GIA versus
166 ELISA indicated the start of a sigmoidal relationship, as previously seen with *P. falciparum* blood-
167 stage vaccines (*9*) (**fig. S6**).

168 **Delayed PvDBPII/M-M vaccination slowed parasite multiplication rate after CHMI.**

169 Following blood-stage CHMI with the heterologous PvW1 clone of *P. vivax*, all volunteers developed
170 parasitemia and received antimalarial treatment after reaching protocol specified malaria diagnostic
171 criteria (**Fig. 4A**, **tables S6 to S8**). Volunteers administered the PvDBPII/M-M vaccine, but not VV-
172 PvDBPII, had significantly lower parasite multiplication rate (PMR) as compared to controls (**table**
173 **S9**, p=0.01). Post-hoc analysis showed that this was due to the delayed dosing regimen group of
174 PvDBPII/M-M, who had a significantly lower median PMR of 3.2-fold growth per 48 hours (range
175 2.3 to 4.3) compared to the unvaccinated controls (median PMR of 6.8-fold growth per 48 hours
176 [range 4.0 to 11.1], p<0.001) (**Fig. 4B**). This equated to a 53% reduction in median PMR and was
177 reflected in a 7-day delay in median time to reach malaria diagnosis, from 15.5 days in controls to
178 22.5 days in vaccinees (**fig. S7**). Exploratory analysis of $\log_{10}$ cumulative parasitemia (LCP) gave
179 concordant results and showed significantly lower LCP in those administered PvDBPII/M-M in the
180 delayed dosing regimen as compared to controls (**Fig. 4C**, p=0.01). PMR and LCP significantly
181 correlated (**fig. S8**, p=0.01). The other vaccination regimens showed no impact on any outcome
182 measure. PMR did not differ by Duffy blood group serophenotype, after adjusting for vaccination
183 group (**table S10**). Parasitemia at the time of malaria diagnosis was consistent across all groups (**fig.**

184 **S9**). The frequency and severity of solicited malaria symptoms, pyrexia and hematological and
185 biochemical laboratory abnormalities occurring during CHMI were similar between vaccinees and the
186 control volunteers (**fig. S10**).

187 **Antibody readouts after vaccination correlated with in vivo parasite growth inhibition.**
188 We assessed the relationship between measurements of vaccine immunogenicity pre-CHMI with in
189 vivo growth inhibition (IVGI) observed during CHMI. IVGI was calculated for each vaccinated
190 individual as the percentage reduction in PMR relative to the mean PMR in the unvaccinated controls.
191 The mean IVGI in those administered PvDBPII/M-M in the delayed dosing regimen was 51% (range
192 36% to 66%). We found no association between IVGI and vaccine-induced $CD4^+$ T cell IFN-γ
193 responses (**Fig. 5A**). In contrast, correlations were observed between IVGI and all three antibody
194 readouts: anti-PvDBPII (PvW1) total IgG serum antibody enzyme-linked immunosorbent assay
195 (ELISA; **Fig. 5B**), BIA using PvW1 sequence PvDBPII protein (**Fig. 5C**), and in vitro GIA using
196 purified IgG against *P. knowlesi* parasites expressing the PvDBP PvW1 allele (**Fig. 5D**).
197

198 **Discussion**
199 The interaction between PvDBP and its host receptor DARC/Fy is critical for *P. vivax* invasion of
200 reticulocytes, which explains the natural resistance of Duffy-negative individuals to *P. vivax* blood-
201 stage infection (*5*). Structural studies have demonstrated that region II within PvDBP binds to DARC
202 (*10*) and numerous immuno-epidemiological studies (*11, 12*) and preclinical vaccine models (*13, 14*)
203 have supported the hypothesis that vaccine-induced anti-PvDBPII antibodies could inhibit blood-stage
204 *P. vivax* parasite growth. Here we present the clinical vaccine trial results confirming this concept.
205

206 The Phase I/IIa trials reported here tested two different vaccine platforms to deliver the PvDBPII
207 antigen. Results indicated no safety concerns and both vaccine formulations induced immune
208 responses to PvDBPII. However, following CHMI, only the protein-in-adjuvant vaccine PvDBPII/M-
209 M, given in a delayed 0-1-14 month dosing regimen, inhibited parasite growth. The average reduction

of parasite growth by 51% confirms that vaccines targeting PvDBPII can induce anti-parasitic immunity. In comparison, the most advanced blood-stage *P. falciparum* vaccine, RH5.1/AS01$_B$, achieved much higher in vitro GIA but reduced parasite growth in vivo by only around 20% following CHMI (*9*). The reduction in parasite growth in those who received PvDBPII/M-M in the delayed dosing regimen was reflected in a 7-day delay to reach malaria diagnosis and associated delay in development of malaria symptoms. However, there was no reduction in the severity of clinical malaria in these vaccinees compared to controls once they reached the protocol specified malaria diagnostic criteria.

Parasite growth rate during CHMI was calculated from the slope of a linear model fitted to $\log_{10}$ transformed quantitative polymerase chain reaction (qPCR) data, the method we have used for blood-stage CHMI studies to date (*8, 9, 15, 16*). PMR is based only on the rate of parasite growth after parasitemia is detectable by qPCR and does not differentiate between differences in time to reach detectable parasitemia. We therefore also calculated $\log_{10}$ cumulative parasitemia, a potentially more differentiating measure as it is affected by both the time to reach detectable parasitemia and the rate of parasite growth. In the future, more effective vaccines could control and clear parasitemia and result in non-linear parasite growth, in which case PMR may also not be the most appropriate metric to measure the degree of parasite growth. Of note the number of parasites administered during blood-stage CHMI are $\log_{10}$-fold smaller than the number of merozoites that are estimated to emerge from the liver during natural infection, therefore a longer time to patent parasitemia may be seen following CHMI as compared to natural infection. Nevertheless, the blood-stage CHMI model provides a robust means to detect relatively small reductions in PMR, which can be useful in identifying vaccine candidates with partial efficacy during early stages of clinical development (*15*).

A previous study has suggested that $CD8^+$ T cells are able to kill *P. vivax* infected reticulocytes (*17*). In our vaccine trials, neither vaccine formulation induced a substantial antigen-specific IFN-γ^+ $CD8^+$

T cell response. IFN-γ^+ $CD4^+$ T cell responses to vaccinations were observed, but there was no association between the magnitude of the response with parasite growth during CHMI. We also observed no effect of the Duffy blood group serophenotype on parasite multiplication rate, contrary to reports from field studies (*18*), although the number of volunteers in our studies was small. In contrast, our results indicate that the observed anti-parasitic immunity is antibody mediated, as evidenced by the association between in vivo parasite growth inhibition and three in vitro readouts of vaccine-induced antibodies: anti-PvDBPII-specific responses (measured by ELISA and functional BIA) and anti-parasitic GIA. These data provide important new benchmarks that link these assay readouts with in vivo outcome. The vaccine-induced in vitro GIA observed in these trials are modest, with median GIA of 29% with 10 mg/mL total IgG in the delayed dosing PvDBPII/M-M group. This is in contrast to much higher GIA achieved recently with the blood-stage P. falciparum vaccine RH5.1/$AS01_B$, where median in vitro GIA of about 70% (range of about 60 to 90%) were observed in vaccinated healthy UK adults (*9*).

Our results also indicate that substantial gains in vaccine-induced antibodies can be achieved through modulation of delivery regimen. The delayed 0-1-14 month dosing regimen with PvDBPII/M-M showed improved immunogenicity, which translated into greater efficacy, as compared to the identical vaccine given in a 0-1-2 month regimen. The delayed dosing regimen in this study induced higher peak PvDBPII-specific antibody titers and more potent antibodies as measured by in vitro BIA and GIA, compared to monthly dosing of the PvDBPII/M-M vaccine. The greater binding inhibition may be due to improved antibody avidity, as has also been observed in the delayed dosing regimen of the *P. Falciparum* vaccine RH5.1/$AS01_B$ (*9*). Further immunological analyses from that study suggested that the mechanism for the improvement was greater somatic hypermutation in B cell receptors in the delayed dosing group as compared to the monthly dosing group (*19*) and similar mechanisms could be acting in in the study reported here. Overall our data add to growing evidence that delayed dosing can improve vaccine-induced antibody responses, as has been seen with a variety

of vaccine delivery technologies including those targeting *P. falciparum* and severe acute respiratory syndrome coronavirus 2 (SARS-CoV-2) (*9, 20-22*). However, the very long interval between vaccinations in the 0-1-14 month regimen used in this study would be difficult to implement in the field. The effectiveness of delayed dosing regimens with shorter intervals, such as 0-1-6 months, that could be more easily deployed should now be tested, and in vitro GIA could be used as a surrogate for in vivo outcome to systematically screen a variety of dosing regimens.

Apart from direct inhibition of ligand-receptor binding, vaccine-induced antibodies may mediate inhibition of parasites in vivo through Fc receptor-mediated functions, which are not measured by the standardized GIA assay. Further immunological analyses on larger cohorts to measure a variety of antibody functions could help determine which features in the delayed dosing regimen group are associated with in vivo growth inhibition. This includes measurements of antibody avidity and affinity, the quantity of major anti-PvDBPII specific antibody isotypes and subclasses and the capacity of antibodies to bind Fc receptors and activate different effector cells and complement. In a systems serology analysis of the *P. falciparum* RH5.1/AS01$_B$ vaccine trial, the anti-RH5 IgA1 response was associated with challenge outcome (*9*). This suggests that other vaccine-induced immune mechanisms, apart from inhibition of erythrocyte invasion by IgG as measured by the GIA assay, may be acting to inhibit merozoites and could explain the only moderate correlation of GIA with in vivo parasite inhibition observed in the studies reported here.

A limitation of our trials is the small number of volunteers in each vaccination group due to withdrawals that occurred during the roughly 1 year trial halt secondary to the COVID-19 pandemic, which also necessitated changes to the vaccination regimens partway through the trials. After withdrawals of volunteers during the trial halt, the six volunteers who remained in the study and received the delayed dosing regimen of PvDBPII/M-M followed by CHMI were all female. This may be a confounding factor if females responded better than males to vaccination.

Another limitation is that our studies only used a single clone of *P. vivax* (PvW1) to assess vaccine efficacy. However, the PvW1 clone was recently isolated from a patient in Thailand and thus represents a currently circulating isolate (*8*). It also provided a heterologous challenge to the vaccine-induced responses raised against the SalI allele of PvDBPII. PvDBPII is highly polymorphic with distinct polymorphisms found in parasites from different geographical locations. The 10 polymorphisms in the PvDBP PvW1 allele as compared to the SalI allele are mostly non-conservative amino acid changes and are all found at positions at which polymorphisms occur at high frequency worldwide, including in the highly variant immunodominant 'DEK' epitope (*23*). In the studies reported here binding inhibition and GIA to the PvW1 allele of PvDBPII were well correlated with responses to the SalI allele. Along with the efficacy results, these data indicate that human immunization with PvDBPII can raise antibodies that recognize conserved epitopes within diverse PvDBPII variants. It will nonetheless be important for future studies to test the efficacy of PvDBPII-based vaccines against other heterologous *P. vivax* strains from different geographic locations, strains with PvDBP gene copy number variation (*24*), and parasites that infect Duffy-negative individuals (*25*).

Overall, this study represents an advance for the *P. vivax* blood-stage malaria vaccine field by confirming that vaccine-induced anti-PvDBPII immune responses can impact *P. vivax* growth in malaria-naïve individuals in vivo. Next steps will include CHMI or field efficacy trials of PvDBPII/M-M in malaria-endemic populations. Previous studies have shown that individuals in *P. vivax* endemic areas can acquire anti-PvDBPII antibody responses with increasing exposure, although only a minority of individuals develop high PvDBPII-DARC binding inhibitory antibody titers (*11*). Higher binding inhibition antibodies have been associated with delay in time to re-infection (*11*) and lower parasitemia during re-infection (*12, 26*). Vaccination with PvDBPII may enhance these pre-

existing anti-malarial antibody responses in endemic populations or alternatively pre-existing anti-PvDBP antibodies may inhibit the response to vaccination.

In parallel, avenues to improve vaccine efficacy should be explored. Given that both of the PvDBPII vaccine candidates tested here were designed over 10 years ago, there is potential to rationally improve PvDBP vaccine immunogen design. Further studies to identify the epitopes or regions within this vaccine that elicit the most potent, strain-transcending antibodies will inform which responses need to be elicited in future vaccines (*27*). Approaches to focus the vaccine immune response include retaining only the most potent region of the vaccine immunogen or masking variant immunodominant epitopes that elicit only strain-specific responses (*28*). Use of newer and potentially more immunogenic vaccine platforms such as virus-like particles or mRNA may also improve vaccine efficacy. Looking beyond PvDBP, identifying new blood-stage antigen combinations that can elicit higher GIA (*29, 30*) and combining blood-stage vaccine with those targeting other lifecycle stages (*31, 32*) will likely be required to achieve high vaccine efficacy. Our data reported here provide the framework, with defined benchmark values of anti-PvDBPII antibodies and GIA versus IVGI, to guide rational design and delivery of next-generation blood-stage vaccines to protect against *P. vivax* malaria.

Materials and Methods

Study Design

Two Phase I/IIa vaccine efficacy trials (VAC071, VAC079) and a CHMI trial (VAC069) were conducted in parallel at a single site in the UK (Centre for Clinical Vaccinology and Tropical Medicine, University of Oxford). VAC071 was an open label trial to assess the ChAd63 and MVA viral-vectored vaccines encoding PvDBPII (VV-PvDBPII) (ClinicalTrials.gov number NCT04009096). VAC079 was also an open label trial and assessed the protein vaccine PvDBPII in

Matrix-M adjuvant (PvDBPII/M-M) (ClinicalTrials.gov number NCT04201431). Unvaccinated infectivity controls were enrolled into the VAC069 trial (ClinicalTrials.gov number NCT03797989). Eligible volunteers were healthy, Duffy-positive, malaria-naïve adults, aged 18 to 45 years in the vaccine trials and 18 to 50 years in the VAC069 trial. Full volunteer inclusion and exclusion criteria are found in the supplementary methods. The original planned sample size was 15 volunteers for each vaccine trial. Vaccinations were interrupted in 2020 due to the COVID-19 pandemic. Following the trial halt of around 1 year and withdrawal of volunteers during this period, the trial was amended to allow completion of vaccinations of returning volunteers and to enroll new volunteers to undergo the original vaccination regimens. Vaccinees who completed their vaccinations regimens underwent CHMI at 2 to 4 weeks after their final vaccination, in parallel with infectivity controls from the VAC069 trial. Final sample sizes of volunteers undergoing CHMI were lower than planned due to withdrawals during the COVID-19 pandemic and difficulty with recruitment. The primary objective in both vaccine trials was to determine the efficacy of the vaccines by comparing the PMR during CHMI in vaccinees to the PMR in infectivity controls. Secondary objectives were to assess the safety and humoral and cellular immunogenicity of the vaccines and determine immunological readouts for association with a reduced parasite multiplication rate.

Trial oversight

The trials were designed and conducted at the University of Oxford and received ethical approval from UK National Health Service Research Ethics Services. The VAC071 and VAC079 vaccine trials were approved by the UK Medicines and Healthcare products Regulatory Agency. All participants provided written informed consent and the trials were conducted according to the principles of the current revision of the Declaration of Helsinki 2008 and ICH guidelines for Good Clinical Practice.

Vaccines

ChAd63 PvDBPII is a recombinant replication-defective chimpanzee adenovirus serotype 63 and MVA PvDBPII is a modified vaccinia virus Ankara vector, both encoding PvDBPII (SalI allele) (*6*). Recombinant PvDBPII protein (SalI allele) was produced in *Escherichia coli* to Good Manufacturing Practices at Syngene International (*7*). Matrix-M is a saponin-based adjuvant provided by Novavax AB which is licensed for use in their COVID-19 vaccine (Nuvaxovid). All vaccinations were administered intramuscularly into the deltoid muscle. ChAd63 PvDBPII was administered at a dose of $5x10^{10}$ viral particles (vp); MVA PvDBPII was administered at a dose of $2x10^{8}$ plaque forming units (pfu); and PvDBPII protein was administered at 50 μg, mixed with 50 μg Matrix-M. In the VAC071 trial, ChAd63 PvDBPII was administered at day 0, followed by MVA PvDBPII at 2 months. Vaccinations in group 2 volunteers were interrupted by the COVID-19 pandemic and following a trial halt and amendment to the trial protocol, returning volunteers received a second dose of ChAd63 PvDBPII at 17 months, followed by MVA PvDBPII at 19 months. In the VAC079 trial, PvDBPII was administered at 0, 1 and 2 months. Vaccinations in group 1 volunteers were interrupted by the COVID-19 pandemic and after a trial halt, returning volunteers received their third vaccination at 14 months.

Vaccine safety and immunogenicity

Following each vaccination, local and systemic adverse events (AEs) were self-reported by participants for 7 days using electronic diaries. Unsolicited and laboratory AEs were recorded for 28 days after each vaccination. Serious adverse events (SAEs) were recorded throughout the study period. Details on assessment of severity grading and causality of AEs are provided in the supplemental materials. Post-vaccination clinic reviews were conducted at days 1, 3, 7, 14 and 28 after each vaccination during which observations were taken, adverse events were elicited and blood was taken for hematology, biochemistry and immunology tests.

Total anti-PvDBPII IgG serum concentrations were assessed over time by ELISA using standardized methodology (*6, 9*). BIA which block the interaction of recombinant PvDBPII to DARC in vitro, were assessed in serum using an ELISA-based assay (*6*). In vitro GIA of 10 mg/mL purified total IgG was measured using a transgenic *P. knowlesi* parasite line expressing the PvDBP PvW1 allele (**fig. S11**), modified from a previous version expressing PvDBP SalI allele (*33*). The frequencies of IFN-γ^+ PvDBPII-specific (SalI allele) $CD4^+$ and $CD8^+$ effector memory T cells were measured using flow cytometry.

Controlled human malaria infection

Vaccinees underwent CHMI 2 to 4 weeks following their final vaccination and in parallel with unvaccinated infectivity controls in the VAC069 study. Blood-stage CHMI was initiated by intravenous injection of blood infected with the PvW1 clone of *P. vivax,* which originated from Thailand (*8*). PvW1 possesses a single copy of the PvDBP gene and its PvDBPII sequence is heterologous to SalI (*8*) (**fig. S12**). On the day of CHMI, aliquots of 0.5 mL cryopreserved PvW1 infected blood were thawed and each participant was challenged with a 1:10 dilution of one aliquot by intravenous injection into the forearm (*8*). One dose of the 1:10 diluted inoculum contained between 165 to 217 genome copies (gc) of *P. vivax* as quantified by qPCR, which will be an overestimate of the number of live viable parasites administered per volunteer.

From day 6 or 7 post-CHMI, participants were reviewed in clinic once to twice daily for symptoms of malaria and blood parasitemia was measured in real time by qPCR of the 18S ribosomal RNA gene (*8*). Laboratory staff carrying out qPCR were blinded to the volunteer study group and clinic staff were blinded to the qPCR result of volunteers until qPCR reached malaria diagnostic criteria. Volunteers were commenced on antimalarial treatment if they had substantial malaria symptoms and parasitemia ≥5,000 genome copies (gc)/mL; or if parasitemia reached ≥10,000 gc/mL irrespective of

symptoms. Positive thick film microscopy was also included in the malaria diagnostic criteria in the CHMI trial in 2019 but was removed from later phases (**Fig. 1**). Treatment was with Riamet (60-hour course of artemether/lumefantrine) or Malarone (3-day course of atovaquone/proguanil hydrochloride). Outpatient review continued until completion of antimalarial treatment. Further follow-up visits took place at 2 and 3 months after the day of challenge for all volunteers, and 9 months after challenge in vaccinees only.

Statistical analysis

For the primary efficacy analysis, pairwise comparison of qPCR-derived PMR was made between volunteers who received the same vaccine versus pooled data from all infectivity controls across three CHMIs using Mann-Whitney test. Post-hoc analysis comparing PMR between each vaccination regimen and infectivity controls was performed using Kruskal-Wallis test with Dunn's multiple comparison post-test. The mean of three replicate qPCR results for each individual at each timepoint was used to model the PMR for each volunteer. Mean qPCR values that were below the lower limit of quantification (20 gc/mL) were excluded from further analyses. PMR was calculated from the slope of a linear model fitted to $\log_{10}$ transformed qPCR data (*16*). Exploratory analysis of parasite growth was conducted by calculating $\log_{10}$ cumulative parasitemia (LCP) for each individual up to the day on which the first volunteer reached malaria diagnostic criteria across all CHMIs.

Data were analyzed using GraphPad Prism version 8.3.1 for Windows (GraphPad Software Inc) and statistical tests are indicated in the text. Comparisons between more than two groups were performed using Kruskal-Wallis test with Dunn's multiple comparison post-test. Correlations were assessed using Spearman's rank correlation.

List of Supplementary Materials

Materials and Methods

Figures S1 to S12

Tables S1 to S10

MDAR Reproducibility Checklist

Data file S1

References

1. W. H. Organisation, "World Malaria Report," (2021).
2. R. N. Price, R. J. Commons, K. E. Battle, K. Thriemer, K. Mendis, Plasmodium vivax in the Era of the Shrinking P. falciparum Map. *Trends Parasitol* **36**, 560-570 (2020).
3. S. J. Draper *et al.*, Malaria Vaccines: Recent Advances and New Horizons. *Cell Host Microbe* **24**, 43-56 (2018).
4. C. E. Chitnis, L. H. Miller, Identification of the erythrocyte binding domains of Plasmodium vivax and Plasmodium knowlesi proteins involved in erythrocyte invasion. *J Exp Med* **180**, 497-506 (1994).
5. L. H. Miller, S. J. Mason, D. F. Clyde, M. H. McGinniss, The resistance factor to Plasmodium vivax in blacks. The Duffy-blood-group genotype, FyFy. *N Engl J Med* **295**, 302-304 (1976).
6. R. O. Payne *et al.*, Human vaccination against Plasmodium vivax Duffy-binding protein induces strain-transcending antibodies. *JCI Insight* **2**, (2017).
7. K. Singh *et al.*, Malaria vaccine candidate based on Duffy-binding protein elicits strain transcending functional antibodies in a Phase I trial. *NPJ Vaccines* **3**, 48 (2018).
8. A. M. Minassian *et al.*, Controlled human malaria infection with a clone of Plasmodium vivax with high quality genome assembly. *JCI Insight*, (2021).
9. A. M. Minassian *et al.*, Reduced blood-stage malaria growth and immune correlates in humans following RH5 vaccination. *Med (N Y)* **2**, 701-719 e719 (2021).
10. J. D. Batchelor *et al.*, Red blood cell invasion by Plasmodium vivax: structural basis for DBP engagement of DARC. *PLoS Pathog* **10**, e1003869 (2014).
11. V. C. Nicolete, S. Frischmann, S. Barbosa, C. L. King, M. U. Ferreira, Naturally Acquired Binding-Inhibitory Antibodies to Plasmodium vivax Duffy Binding Protein and Clinical Immunity to Malaria in Rural Amazonians. *J Infect Dis* **214**, 1539-1546 (2016).
12. C. L. King *et al.*, Naturally acquired Duffy-binding protein-specific binding inhibitory antibodies confer protection from blood-stage Plasmodium vivax infection. *Proc Natl Acad Sci U S A* **105**, 8363-8368 (2008).
13. M. Arevalo-Herrera *et al.*, Immunogenicity and protective efficacy of recombinant vaccine based on the receptor-binding domain of the Plasmodium vivax Duffy binding protein in Aotus monkeys. *Am J Trop Med Hyg* **73**, 25-31 (2005).
14. S. Gupta *et al.*, Targeting a Reticulocyte Binding Protein and Duffy Binding Protein to Inhibit Reticulocyte Invasion by Plasmodium vivax. *Sci Rep* **8**, 10511 (2018).
15. R. O. Payne *et al.*, Demonstration of the Blood-Stage Plasmodium falciparum Controlled Human Malaria Infection Model to Assess Efficacy of the P. falciparum Apical Membrane Antigen 1 Vaccine, FMP2.1/AS01. *J Infect Dis* **213**, 1743-1751 (2016).
16. A. D. Douglas *et al.*, Comparison of modeling methods to determine liver-to-blood inocula and parasite multiplication rates during controlled human malaria infection. *J Infect Dis* **208**, 340-345 (2013).
17. C. Junqueira *et al.*, Cytotoxic CD8(+) T cells recognize and kill Plasmodium vivax-infected reticulocytes. *Nat Med* **24**, 1330-1336 (2018).
18. C. L. King *et al.*, Fy(a)/Fy(b) antigen polymorphism in human erythrocyte Duffy antigen affects susceptibility to Plasmodium vivax malaria. *Proc Natl Acad Sci U S A* **108**, 20113-20118 (2011).
19. C. M. Nielsen *et al.*, Delayed boosting improves human antigen-specific Ig and B cell responses to the RH5.1/AS01B malaria vaccine. *JCI Insight* **8**, (2023).
20. J. A. Regules *et al.*, Fractional Third and Fourth Dose of RTS,S/AS01 Malaria Candidate Vaccine: A Phase 2a Controlled Human Malaria Parasite Infection and Immunogenicity Study. *J Infect Dis* **214**, 762-771 (2016).

21. A. Flaxman *et al.*, Reactogenicity and immunogenicity after a late second dose or a third dose of ChAdOx1 nCoV-19 in the UK: a substudy of two randomised controlled trials (COV001 and COV002). *Lancet* **398**, 981-990 (2021).
22. R. P. Payne *et al.*, Immunogenicity of standard and extended dosing intervals of BNT162b2 mRNA vaccine. *Cell* **184**, 5699-5714 e5611 (2021).
23. P. Mittal *et al.*, Global distribution of single amino acid polymorphisms in Plasmodium vivax Duffy-binding-like domain and implications for vaccine development efforts. *Open Biol* **10**, 200180 (2020).
24. J. Popovici *et al.*, Amplification of Duffy binding protein-encoding gene allows Plasmodium vivax to evade host anti-DBP humoral immunity. *Nat Commun* **11**, 953 (2020).
25. P. Wilairatana, F. R. Masangkay, K. U. Kotepui, G. De Jesus Milanez, M. Kotepui, Prevalence and risk of Plasmodium vivax infection among Duffy-negative individuals: a systematic review and meta-analysis. *Sci Rep* **12**, 3998 (2022).
26. J. L. Cole-Tobian *et al.*, Strain-specific duffy binding protein antibodies correlate with protection against infection with homologous compared to heterologous plasmodium vivax strains in Papua New Guinean children. *Infect Immun* **77**, 4009-4017 (2009).
27. T. A. Rawlinson *et al.*, Structural basis for inhibition of Plasmodium vivax invasion by a broadly neutralizing vaccine-induced human antibody. *Nat Microbiol* **4**, 1497-1507 (2019).
28. F. B. Ntumngia *et al.*, An engineered vaccine of the Plasmodium vivax Duffy binding protein enhances induction of broadly neutralizing antibodies. *Sci Rep* **7**, 13779 (2017).
29. C. T. Franca *et al.*, Identification of highly-protective combinations of Plasmodium vivax recombinant proteins for vaccine development. *Elife* **6**, (2017).
30. R. Mazhari *et al.*, Identification of novel Plasmodium vivax proteins associated with protection against clinical malaria. *Front Cell Infect Microbiol* **13**, 1076150 (2023).
31. M. Arevalo-Herrera *et al.*, Randomized clinical trial to assess the protective efficacy of a Plasmodium vivax CS synthetic vaccine. *Nat Commun* **13**, 1603 (2022).
32. J. W. Bennett *et al.*, Phase 1/2a Trial of Plasmodium vivax Malaria Vaccine Candidate VMP001/AS01B in Malaria-Naive Adults: Safety, Immunogenicity, and Efficacy. *PLoS Negl Trop Dis* **10**, e0004423 (2016).
33. F. Mohring *et al.*, Rapid and iterative genome editing in the malaria parasite Plasmodium knowlesi provides new tools for P. vivax research. *Elife* **8**, (2019).
34. R. O. Payne *et al.*, Human vaccination against Plasmodium vivax Duffy-binding protein induces strain-transcending antibodies. *JCI Insight* **2**, 93683 (2017).
35. K. Singh *et al.*, Malaria vaccine candidate based on Duffy-binding protein elicits strain transcending functional antibodies in a Phase I trial. *NPJ Vaccines* **3**, 48 (2018).
36. F. Mohring *et al.*, Rapid and iterative genome editing in the malaria parasite Plasmodium knowlesi provides new tools for P. vivax research. *Elife* **8**, (2019).
37. F. Mohring, M. N. Hart, A. Patel, D. A. Baker, R. W. Moon, CRISPR-Cas9 Genome Editing of Plasmodium knowlesi. *Bio Protoc* **10**, e3522 (2020).
38. E. M. Malkin *et al.*, Phase 1 clinical trial of apical membrane antigen 1: an asexual blood-stage vaccine for Plasmodium falciparum malaria. *Infect Immun* **73**, 3677-3685 (2005).
39. A. M. Minassian *et al.*, Controlled human malaria infection with a clone of Plasmodium vivax with high quality genome assembly. *JCI Insight*, (2021).
40. J. S. McCarthy *et al.*, Experimentally induced blood-stage Plasmodium vivax infection in healthy volunteers. *J Infect Dis* **208**, 1688-1694 (2013).
41. A. D. Douglas *et al.*, Comparison of modeling methods to determine liver-to-blood inocula and parasite multiplication rates during controlled human malaria infection. *J Infect Dis* **208**, 340-345 (2013).

Acknowledgments

The authors are grateful for the assistance of Aabidah Ali, Megan Baker, Duncan Bellamy, Nicholas Byard, Federica Cappuccini, Hannah Davies, Francesca Donnellan, Amy Flaxman, Julie Furze, Michelle Fuskova, Daniel Jenkins, Kimberly Johnson, Kathryn Jones, Reshma Kailath, Colin Larkworthy, Fernando Ramos Lopez, Meera Madhavan, Rebecca Makinson, Daniel Marshall-Searson, Celia Mitton, Abigail Platt, Jack Quaddy, Raquel Lopez Ramon, Indra Rudiansyah, Hannah Scott, Merin Thomas, Cheryl Turner, Nicola Turner, Marta Ulaszewska, Chris Williams, Rhea Zambellas (Jenner Institute, University of Oxford); Robert Smith, Eleanor Berrie, Helena Parracho and Richard Tarrant (Clinical Biomanufacturing Facility, University of Oxford); Sally Pelling-Deeves for arranging contracts (University of Oxford); Julie Staves and the Haematology Laboratory (Oxford University Hospitals NHS Foundation Trust); Narimane Nekkab and Melissa Penny for statistical modelling (Swiss Tropical and Public Health Institute); Xin Xue Liu for statistical advice (Oxford Vaccine Group, University of Oxford); Karin Lövgren Bengtsson (Novavax); Nongnuj Maneechai, Tianrat Piteekan, Nattawan Rachaphaew, Wanlapa Roobsoong, Jetsumon Sattabongkot, Nick Day (Mahidol Vivax Research Unit, Thailand); members of the MultiViVax Scientific Advisory Board; past members of the Malaria Group, ICGEB including Sanjay Singh, Kailash Pandey, Shams Yazdani, Ahmed Rushdi Shakri, Dhiraj Hans, Pankaj Gupta and Rukmini Bharadwaj; past members of MVDP, including Kavita Singh, Gaurav Pandey, Shantanu Mehta and Rajender Jena, for playing key roles in development of the PvDBPII protein vaccine; and all the study volunteers.

Funding

The VAC069 and VAC071 trials were funded by the European Union's Horizon 2020 research and innovation program under grant agreement 733073 for MultiViVax. The VAC079 trial was funded by the Wellcome Trust Malaria Infection Study in Thailand (MIST) program (212336/Z/18/Z). This work was also supported in part by the UK Medical Research Council (MRC) [G1100086] and the National Institute for Health Research (NIHR) Oxford Biomedical Research Centre (BRC). DJML

holds a NIHR Academic Clinical Fellowship. The views expressed are those of the authors and not necessarily those of the NHS, the NIHR or the Department of Health. The GIA work was supported by the Intramural Program of the National Institutes of Health, National Institute of Allergy and Infectious Diseases. RWM and FM were supported by the UK MRC (Career Development Award MR/M021157/1). Development of PvDBPII as a vaccine candidate was supported by grants from the Biotechnology Industry Research Assistance Council (BIRAC), New Delhi and PATH Malaria Vaccine Initiative. MVDP was supported by grants from the Bill and Melinda Gates Foundation and Department of Biotechnology (DBT), Government of India. This work was also supported in part by grants from Agence Nationale de Recherche to CEC (ANR-18- CE15-0026 and ANR 21 CE15-0013-01). CEC is supported by the French Government's Laboratoire d'Excellence "PARAFRAP" (ANR-11-LABX-0024-PARAFRAP). FJM was supported by a Fellowship from Ecole Doctorale BioSPC, Université Paris Cité. CMN held a Wellcome Trust Sir Henry Wellcome Postdoctoral Fellowship (209200/Z/17/Z). TAR held a Wellcome Trust Research Training Fellowship (108734/Z/15/Z). SB and SJD are Jenner Investigators and SJD held a Wellcome Trust Senior Fellowship (106917/Z/15/Z).

Author Contributions

MMH, YT, TAR, SES, CEC, AMM and SJD designed the studies. MMH, YT, TAR, NMG, LK, IDP, BK, CG, SHH, DJML, JS and AMM collected the clinical data. JRB, CMN, AML, LDWK, NJE and SES conducted ELISA, flow cytometry and qPCR. FJM and MG-B conducted BIA assays. AD and KM conducted GIA assays. MMH, JRB, CMN, NJE, KM, SES, CEC, AMM and SJD analyzed the data. CH, JMR, VSC, PM, CAL, FM, RWM, KM and CEC contributed reagents, materials and or analysis tools. PM, SB, IJT, AML, JSC, FLN provided trial planning. MMH, JRB, AMM and SJD wrote the paper.

Competing Interests

SJD has consulted to GSK on malaria vaccines, and is an inventor on patent applications relating to adenovirus-based vaccines (PCT/GB2008/001262: Adenoviral Vectors Encoding a Pathogen or Tumour Antigen), and is an inventor on intellectual property licensed by Oxford University Innovation to AstraZeneca. AMM has consulted to GSK on malaria vaccines, and has an immediate family member who is an inventor on patents relating to adenovirus-based vaccines (PCT/GB2008/001262: Adenoviral Vectors Encoding a Pathogen or Tumour Antigen), and is an inventor on intellectual property licensed by Oxford University Innovation to AstraZeneca. CEC is an inventor on patents that relate to binding domains of erythrocyte-binding proteins of *Plasmodium* parasites including PvDBP (patent no. 6962987; Binding domains from Plasmodium vivax and Plasmodium falciparum erythrocyte binding proteins). JMR is an employee of Novavax, developer of the Matrix-M adjuvant and is listed as an inventor on patent application no. PCT/US2022/080334: Methods and compositions for treating and preventing malaria. MMH, NMG, IDP, YT and BK are contributors to intellectual property licensed by Oxford University Innovation to AstraZeneca. All other authors have declared that no conflict of interest exists.

Data and Materials Availability: All data associated with this study are in the paper or supplementary materials. Requests for datasets and materials should be addressed to the corresponding author, aside from requests for transgenic *P. knowlesi* lines, which are available from RWM under a material transfer agreement with the Francis Crick Institute and London School of Hygiene and Tropical Medicine. This research was funded in whole or in part by the Wellcome Trust [Grant number 212336/Z/18/Z], a cOAlition S organization. The author will make the Author Accepted Manuscript (AAM) version available under a CC BY public copyright license.

Figures

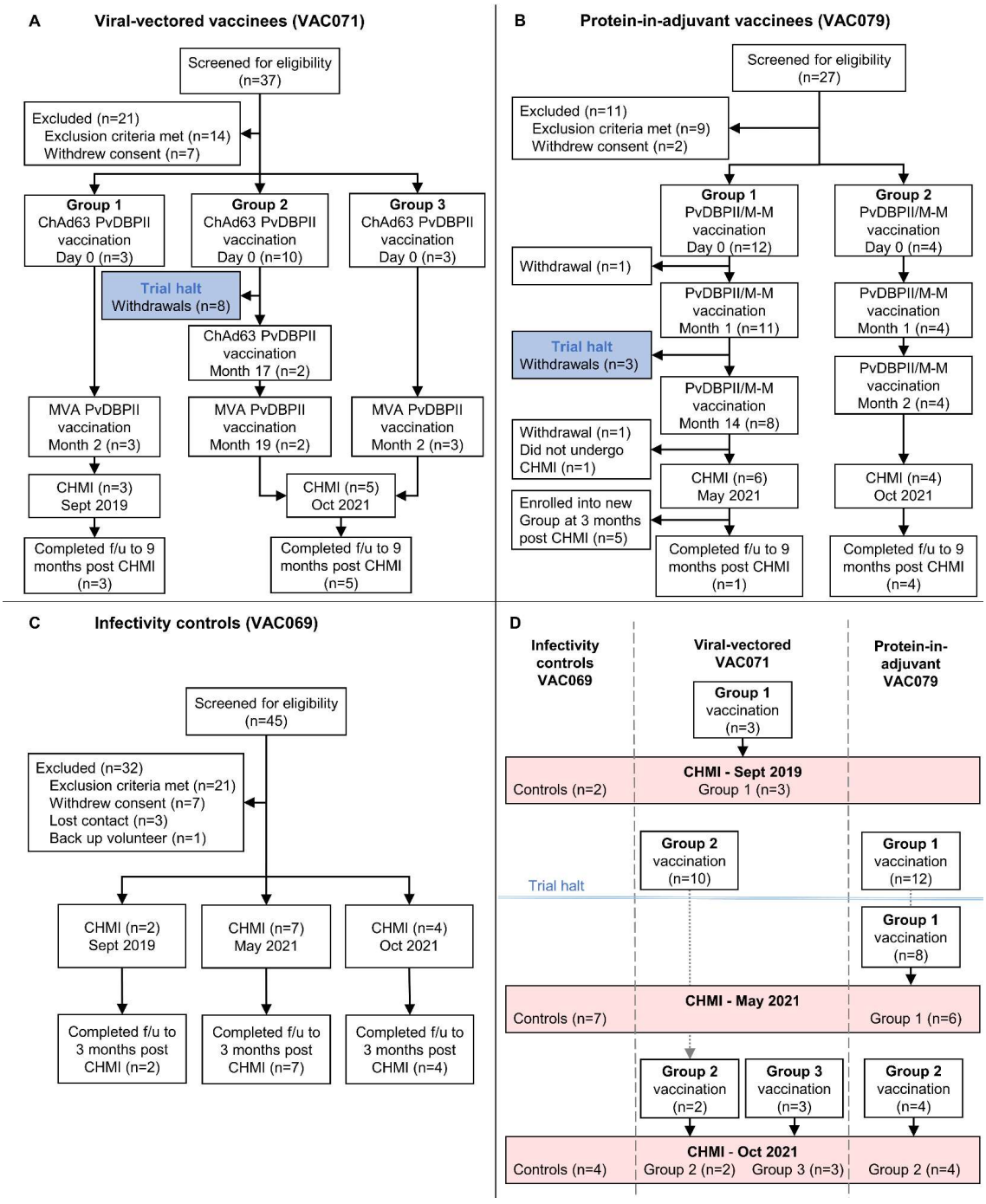

Figure 1. Flow charts of study design and participant recruitment.

(**A**) VAC071 Group 1 participants received the viral-vectored vaccines ChAd63 PvDBPII and MVA PvDBPII 8 weeks apart, followed by CHMI 2 to 4 weeks later. Group 2 received ChAd63 PvDBPII

before the trial was temporarily halted. On restart of the trial, returning participants in Group 2 received a second dose of ChAd63 PvDBPII at 17 months, followed by MVA PvDBPII 8 weeks later. Group 3 participants received the 8-week viral-vectored vaccine regimen and underwent CHMI along with Group 2 volunteers at 2 to 4 weeks after the final vaccination. (**B**) VAC079 participants received protein PvDBPII vaccine in Matrix-M adjuvant (PvDBPII/M-M). Group 1 volunteers received three doses at 0-1-14 months (delayed third dose due to trial halt). Group 2 volunteers received three doses at 0-1-2 months, with CHMI at 2 to 4 weeks after the final vaccination. (**C**) VAC069 participants underwent blood-stage CHMI in three separate stages and acted as infectivity controls for vaccinees undergoing CHMI in parallel. (**D**) Shown is a summary of the three CHMIs. VAC071 Group 1 vaccinees underwent CHMI in parallel with control participants in September 2019. In January 2020 vaccinations commenced in VAC071 and VAC079, before the trials were halted in March 2020. After restart of the VAC079 trial in 2021, Group 1 participants underwent CHMI in parallel with control participants in May 2021. In October 2021, control participants underwent CHMI in parallel with vaccinees from VAC071 Groups 2 and 3 and VAC079 Group 2. f/u, follow-up.

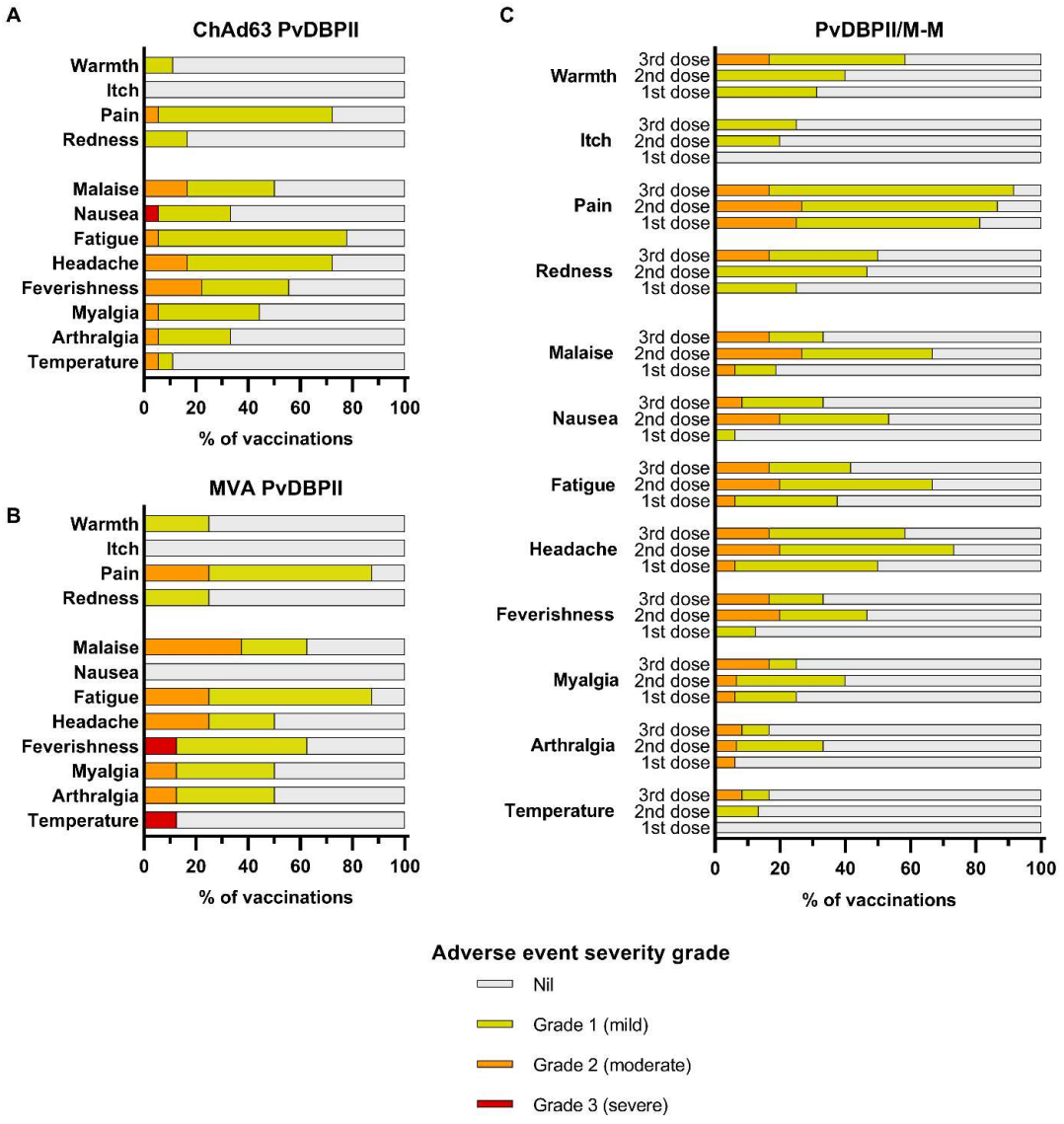

Figure 2. Local and systemic solicited adverse events.

Solicited AEs were recorded by volunteers within 7 days following each vaccination in participant symptom electronic diaries. The maximal severity reported for each AE is shown as a percentage of the number of vaccinations administered. (**A**) ChAd63 PvDBPII AEs are shown; n=18 vaccinations (16 volunteers received one dose, 2 volunteers received a second dose). (**B**) MVA PvDBPII AEs are shown; n=8 vaccinations (8 volunteers received one dose). (**C**) PvDBPII/M-M AEs are shown. AEs reported after first (n=16), second (n=15), and third doses (n=12) are shown.

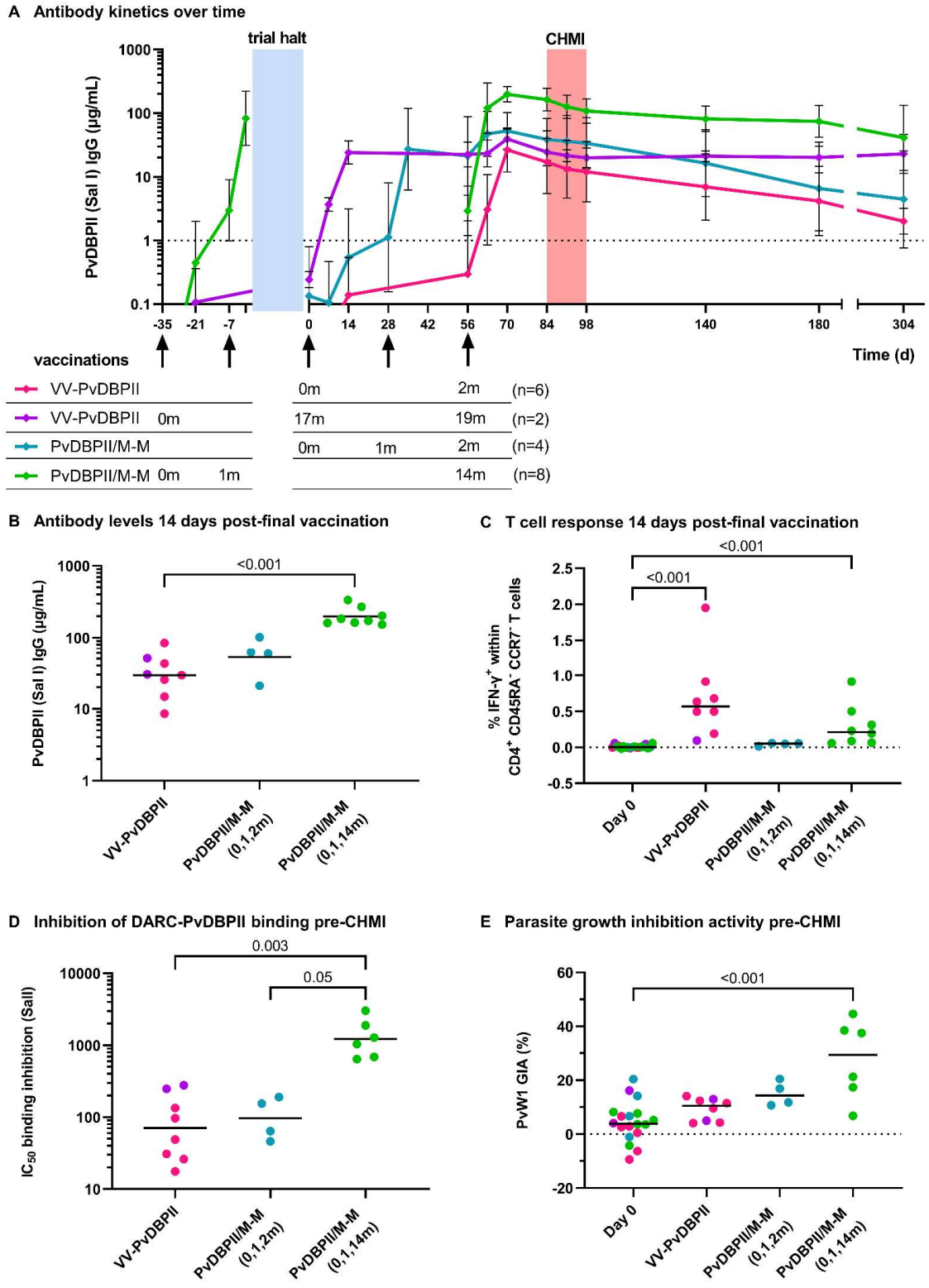

Figure 3. Immunological responses were elicited by PvDBPII vaccinations.

(**A**) Anti-PvDBPII Salvador I (SalI) strain total IgG serum concentrations are shown over time for each vaccination regimen showing geometric mean with standard deviation. Groups are aligned at the time of final vaccination (day 56). Arrows indicate vaccinations with timing of doses in each regimen indicated below in months. VV-PvDBPII indicates viral-vectored vaccines. Blue shading indicates trial halt of about 1 year, vaccinations occurring prior to the trial halt are shown to the left. Red shading indicates period of controlled human malaria infection (CHMI). IgG concentrations below 1 μg/mL, indicated by dotted line, are classified as negative responses but shown for clarity. (**B**) Shown are individual anti-PvDBPII (SalI) total IgG serum concentrations 14 days post-final vaccination with geometric means for each regimen. (**C**) Shown are the percentages of IFN-γ^+ cells within $CD4^+$ $CD45RA^-$ $CCR7^-$ effector memory T cells collected 14 days post-final vaccination following stimulation of peripheral blood mononuclear cells with a pool of PvDBPII (SalI) peptides, with group medians. The frequency of IFN-γ^+ cells in sample-matched unstimulated wells was subtracted to control for non-specific activation. Baseline responses (Day 0) are shown for all volunteers. (**D**) Shown are the dilution factors of individual serum, taken pre-CHMI, required to inhibit DARC-PvDBPII (SalI) binding by 50% (IC_{50}) with geometric means. Baseline responses (Day 0) are shown for all volunteers. (**E**) Shown is the percentage of in vitro growth inhibition activity (GIA) of 10 mg/mL purified total IgG, taken pre-CHMI, against *P. knowlesi* parasites expressing PvDBP PvW1 allele, with medians. Baseline responses (Day 0) are shown for all volunteers. *p* values were calculated by Kruskal-Wallis test with Dunn's multiple comparison post-test.

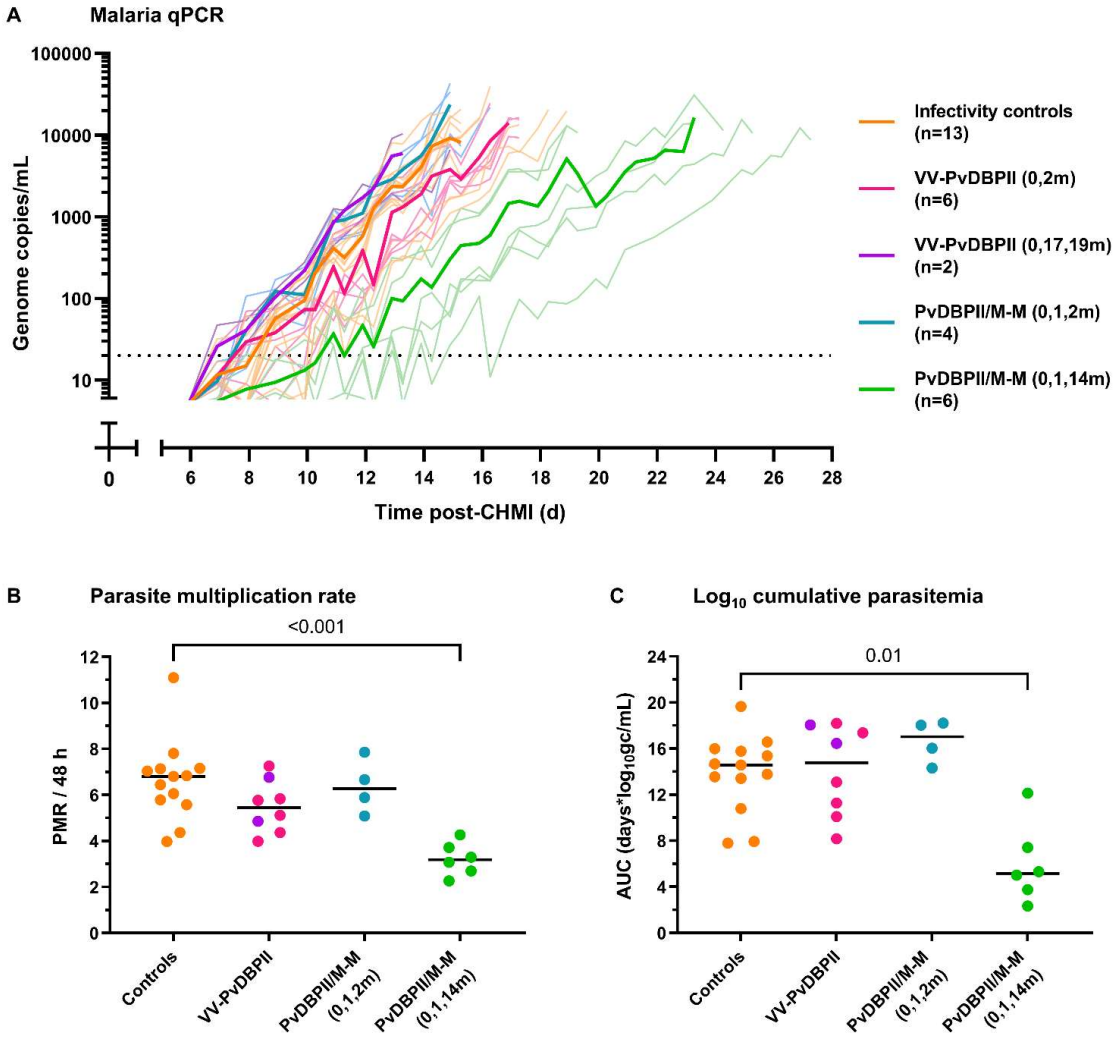

Figure 4. PvDBPII/M-M inhibits growth of *P. vivax* after CHMI.

(**A**) Individual parasitemia over time was measured by qPCR, with group means in bold lines. Timings of vaccinations are shown in brackets in months. On the day of CHMI, volunteers were administered an intravenous injection of *P. vivax* (PvW1 clone) blood-stage parasites. The dotted line indicates the minimum concentration of parasitemia to meet positive reporting criteria (20 genome copies [gc]/mL). (**B**) Shown is a comparison of parasite multiplication rate (PMR) per 48 hours between vaccinees and controls. Individual PMRs are modelled from the qPCR data over time and are shown with group median. (**C**) Shown is a comparison of $\log_{10}$ cumulative parasitemia (LCP) during CHMI between vaccinees and controls with group median. LCP calculated from area under the curve

(AUC) of log_{10}-transformed qPCR over time for each individual, up until day 14 after challenge when the first volunteer reached malaria diagnostic criteria across all CHMIs. *p* values were calculated by Kruskal-Wallis test with Dunn's multiple comparison post-test.

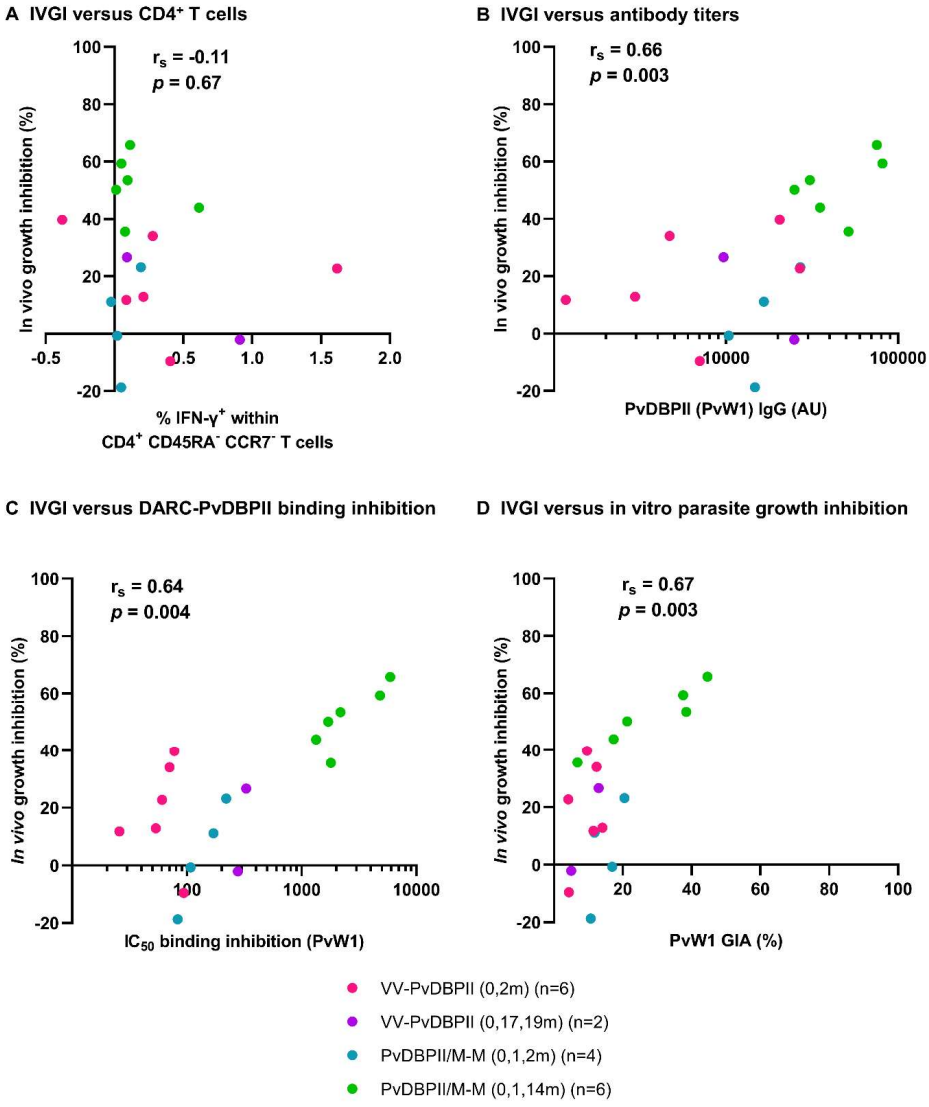

Figure 5. Antibody activity correlates with in vivo parasite growth inhibition.

(**A to D**) The percent of in vivo parasite growth inhibition (IVGI), calculated as % reduction in PMR in vaccinees relative to the mean PMR in infectivity controls were correlated with pre-CHMI measurements of percentage of IFN-γ^+ cells within $CD4^+$ $CD45RA^-$ $CCR7^-$ effector memory T cells (**A**); anti-PvDBPII (PvW1) total IgG serum titers in arbitrary units (AU) (**B**); dilution factor of individual serum required to inhibit DARC-PvDBPII (PvW1) binding by 50% (IC_{50}) (**C**); and (**D**) % in vitro GIA of 10 mg/mL purified total IgG against *P. knowlesi* parasites expressing the PvDBP PvW1 allele. Spearman's rank correlation coefficients and *p* values are shown, n=18.

Supplementary Materials and Methods

Trial approvals

The studies received ethical approval from UK National Health Service Research Ethics Services, (VAC069: Hampshire A Research Ethics Committee, Ref 18/SC/0577; VAC071: Oxford A Research Ethics Committee, Ref 19/SC/0193; VAC079: Oxford A Research Ethics Committee, Ref 19/SC/0330). The vaccine trials were approved by the UK Medicines and Healthcare products Regulatory Agency (VAC071: EudraCT 2019-000643-27; VAC079: EudraCT 2019-002872-14).

Trial inclusion and exclusion criteria

Inclusion and exclusion criteria for both vaccine trials (VAC071, VAC079) are listed below.

Inclusion criteria:

- Healthy adult aged 18 to 45 years.
- Red blood cells positive for the Duffy antigen/chemokine receptor (DARC).
- Normal serum levels of Glucose-6-phosphate dehydrogenase (G6PD).
- Able and willing (in the Investigator's opinion) to comply with all study requirements.
- Willing to allow the Investigators to discuss the volunteer's medical history with their General Practitioner.
- Women only: Must practice continuous effective contraception for the duration of the study
- Agreement to permanently refrain from blood donation.
- Written informed consent to participate in the trial.
- Reachable (24/7) by mobile phone during the period between controlled human malaria infection (CHMI) and completion of all antimalarial treatment.
- Willing to take a curative anti-malarial regimen following CHMI.
- Willing to reside in Oxford for the duration of the study, until antimalarials have been completed.
- Answer all questions on the informed consent quiz correctly.

Exclusion criteria:

- History of clinical malaria (any species).
- Travel to a clearly malaria endemic locality during the study period or within the preceding six months.
- Current or planned treatment with long-acting immune-modifying drugs at any time during the study period (e.g. infliximab).
- Chronic use of antibiotics with antimalarial effects (e.g. tetracyclines for dermatologic patients, trimethoprim-sulfamethoxazole for recurrent urinary tract infections, or others).
- Weight less than 50kg, as measured at the screening visit.
- Receipt of immunoglobulins within the three months prior to planned administration of the vaccine candidate.
- Receipt of blood products (e.g., blood transfusion) at any time in the past.

- Peripheral venous access unlikely to allow twice daily blood testing (as determined by the Investigator).
- Receipt of an investigational product in the 30 days preceding enrolment, or planned receipt during the study period.
- Receipt of any vaccine in the 30 days preceding enrollment, or planned receipt of any other vaccine within 30 days preceding or following each study vaccination, with the exception of licensed COVID-19 vaccines, which should not be received within 14 days before or 7 days after any study vaccination.
- Planned receipt of a COVID-19 vaccine between 2 weeks before the day of CHMI until completion of antimalarial treatment.
- Concurrent involvement in another clinical trial or planned involvement during the study period.
- Prior receipt of an investigational vaccine likely to impact on interpretation of the trial data or the *Plasmodium vivax* parasite as assessed by the Investigator.
- History of sickle cell anemia, sickle cell trait, thalassemia or thalassemia trait or any hematological condition that could affect susceptibility to malaria infection.
- Any confirmed or suspected immunosuppressive or immunodeficient state, including HIV infection; asplenia; recurrent, severe infections and chronic (more than 14 days); or immunosuppressant medication within the past 6 months (inhaled and topical steroids are allowed).
- History of allergic disease or reactions likely to be exacerbated by any component of the vaccine, such as egg products, Kathon, aminoglycosides.
- History of allergic disease or reactions likely to be exacerbated by malaria infection.
- History of clinically significant contact dermatitis.
- Any history of anaphylaxis in reaction to vaccinations.
- Pregnancy, lactation or intention to become pregnant during the study.
- Use of medications known to cause prolongation of the QT interval and existing contraindication to the use of Malarone.
- Use of medications known to have a potentially clinically significant interaction with Riamet and Malarone.
- Any clinical condition known to prolong the QT interval.
- History of cardiac arrhythmia, including clinically relevant bradycardia.
- Disturbances of electrolyte balance, e.g. hypokalemia or hypomagnesaemia.
- Family history of congenital QT prolongation or sudden death.
- Contraindications to the use of both of the proposed anti-malarial medications; Riamet Malarone.
- History of cancer (except basal cell carcinoma of the skin and cervical carcinoma in situ).
- History of serious psychiatric condition that may affect participation in the study.
- Any other serious chronic illness requiring hospital specialist supervision.
- Suspected or known current alcohol abuse as defined by an alcohol intake of greater than 25 standard UK units every week.
- Suspected or known injecting drug abuse in the 5 years preceding enrolment.
- Hepatitis B surface antigen (HBsAg) detected in serum.
- Seropositive for hepatitis C virus (antibodies to HCV) at screening, or (unless has taken part in a prior hepatitis C vaccine study with confirmed negative HCV antibodies prior to participation in that study, and negative HCV RNA polymerase chain reaction (PCR) at screening for this study).

- Positive family history in both 1st AND 2nd degree relatives < 50 years old for cardiac disease.
- Volunteers unable to be closely followed for social, geographic, or psychological reasons.
- Any clinically significant abnormal finding on biochemistry or hematology blood tests, urinalysis or clinical examination. In the event of abnormal test results, confirmatory repeat tests will be requested. Procedures for identifying laboratory values meeting exclusion criteria are shown in SOP VC027.
- Any other significant disease, disorder, or finding which may significantly increase the risk to the volunteer because of participation in the study, affect the ability of the volunteer to participate in the study or impair interpretation of the study data.
- Inability of the study team to contact the volunteer's GP to confirm medical history and safety to participate.

Peripheral Blood Mononuclear Cell (PBMC), plasma, and serum preparation

Blood samples were collected into lithium heparin-treated vacutainer blood collection systems. PBMC were frozen in fetal calf serum containing 10% dimethyl sulfoxide and stored in liquid nitrogen. Plasma samples were stored at -80 °C. For serum preparation, blood samples were collected into untreated vacutainers, incubated at room temperature and then the clotted blood was centrifuged for 5 min (750 *x g*). Serum was stored at -80 °C.

Anti-PvDBPII standardized enzyme-linked immunosorbent assay (ELISA)

ELISAs to quantify circulating PvDBPII-specific total IgG responses were performed using standardized methodology, similar to that previously described (*34*). Nunc MaxiSorp ELISA plates (Thermo Fisher) were coated overnight (≥16 h) at 4 °C with 50 µL per well of 2 µg/mL PvDBPII (SalI or PvW1 allele) protein (*34*). Plates were washed 6x with 0.05 % phosphate-buffered saline/Tween (PBS/T) and tapped dry. Plates were blocked for 1 h with 100 µL per well of Starting Block T20 (Thermo Fisher) at 20 °C. Test samples were diluted in blocking buffer (minimum dilution of 1:100), and 50 µL per well was added to the plate in triplicate. Reference serum (made from a pool of high-titer vaccinated donor serum) was diluted in blocking buffer in a three-fold dilution series to form a ten-point standard curve. Three independent dilutions of the reference serum were made to serve as internal controls. The standard curve and internal controls were added to the plate at 50 µL per well in duplicate. Plates were incubated for 2 h at 20 °C and then washed 6x with PBS/T and tapped dry. Goat anti-human IgG–alkaline phosphatase secondary antibody (Merck) was diluted 1:1000 in blocking buffer and 50 µL per well was added. Plates were incubated for 1 h at 20 °C. Plates were washed 6x with PBS/T and tapped dry. 100 µL per well of p-nitrophenyl phosphate alkaline phosphatase substrate (Thermo Fisher) was added, and plates were incubated for approximately 15 min at 20 °C. Optical density at 405 nm (OD_{405}) was measured using an ELx808 absorbance reader (BioTek) until

the internal control reached an OD_{405} of 1.0. The reciprocal of the internal control dilution giving an OD_{405} of 1.0 was used to assign an arbitrary unit (AU) value of the standard. Gen5 ELISA software v3.04 (BioTek) was used to convert the OD_{405} of test samples into AU by interpolating from the linear range of the standard curve fitted to a four-parameter logistic model. Any test samples with an OD_{405} below the linear range of the standard curve at the minimum dilution tested were assigned a minimum AU value of 5.0. These responses in AU are reported in µg/mL for the PvDBPII SalI allele following generation of a conversion factor by calibration-free concentration analysis (CFCA). In short, CFCA was performed using a Biacore X100 instrument, a Biotin CAP chip and X100 control and evaluation software (Cytiva). Purified mono-biotinylated antigen was produced for use in CFCA and chip was regenerated with manufacturer's supplied regeneration and CAP reagents and fresh antigen prior to each application of antibody. Serum samples, from a previous clinical trial (VAC051 (*34*)), with a range of PvDBP antibody responses were diluted and assessed for antigen-specific antibody binding and initial rates of antigen-specific binding at 5 µL/min and 100 µL/min measured and compared to permit measurement of concentration. The CFCA-measured PvDBP-specific antibody concentrations for each individual were analyzed by linear regression with corresponding total IgG ELISA AU data, where slope of the line was used to derive an AU-to-µg/mL conversion factor.

ELISA-based Binding Inhibition Assay

Samples were analyzed for binding inhibitory antibodies (BIA) at the Institut Pasteur, Paris, using previously reported methodology (*35*). Recombinant DARC-Fc (1 µg/mL) was coated on to a 96-well plate overnight at 4 °C in carbonate-bicarbonate buffer. Next day, the plate was blocked for 2 h at 37 °C using 2 % non-fat milk. Recombinant PvDBPII (SalI or PvW1 sequence) in a range of 0.8 to 25 ng/mL was used to generate a PvDBPII standard curve using a four-parameter logistic model. Serum samples were analyzed at dilutions of 1:10 to 1:2430. Each serum dilution was incubated with 25 ng/mL PvDBPII protein at 37 °C for 30 min. The reaction mixture was then added to DARC-Fc coated wells of an ELISA plate and incubated at 37 °C for 1 h. PvDBPII protein bound to recombinant DARC was probed with anti-PvDBPII polyclonal rabbit sera at 37 °C for 1 h and detected with anti-rabbit IgG HRP-conjugated secondary antibody at 37 °C for 1 h. The assay was developed using the two-component chromogenic substrate for peroxidase detection TMB (3,3′,5,5′-tetramethylbenzidine, Life Sciences) for 5 min and the reaction was stopped with phosphoric acid 1M (H_3PO_4). Absorbance was immediately measured at a wavelength of 450 nm. The amount of bound PvDBPII was estimated by converting OD values to protein concentrations using the PvDBPII standard curve. The interpolated protein concentration values were used to calculate percent binding for each serum sample dilution. The percent binding inhibition for each serum dilution was calculated as follows: % Binding Inhibition = 100 - % Binding. The plot of % Binding Inhibition versus serum

dilution was used to find the serum dilution at which 50% binding inhibition (IC_{50}) was achieved. Each assay was performed in duplicate and results from three independent replicates were used to determine average IC_{50}.

Plasmodium knowlesi parasites and growth inhibition activity (GIA) assay

It is not possible to culture blood-stage *P. vivax* long-term in vitro and therefore *P. vivax* parasites cannot be used at scale in GIA assays. Instead a transgenic *P. knowlesi* (a closely related simian malaria species) parasite line was generated, which is adapted to long-term in vitro culture in human red blood cells. We previously generated a transgenic *P. knowlesi* parasite line (*P. knowlesi* PvDBP^{OR}ΔβΔγ), in which the PvDBP SalI allele transgene replaced the native PkDBPα gene, and the PkDBPβ and PkDBPγ genes were also knocked out (*36*). Here, we further modify this line to create a transgenic *P. knowlesi* line expressing the PvDBP PvW1 allele (**fig. S10**). A 20 bp guide sequence (CGA CAT CCT GAA GCA GGA AC) targeting the recodonized PvDBP (SalI) was identified and cloned into the PkCas9/sgRNA vector (pCas9/sg_PvDBPRII(SalI)^{OR}) as previously described (*36, 37*). A donor plasmid, pDonor_PvW1, was created by cloning a synthetic recodonized PvDBP PvW1 allele (GeneArt, Thermo Fisher) into the plasmid pDonor_PkDBPα^{OR}, using SpeI and NotI restriction sites. This created the final vector containing PvDBP PvW1 gene sequence flanked by 5' and 3' homology regions targeting the PkDBPα locus. The donor and guide were transfected into *P. knowlesi* PvDBP^{OR}ΔβΔγ using previously described methods (*36*). The resultant transfectants were cloned by limiting dilution and genotyped by PCR as described previously using diagnostic oligos for WT PvDBPRII^{OR} locus (ol186 fwd-CAC GAT TTG TGT ACT TAT AGA ATC AAT TTT TCC TT and ol189 rev-CGT TCT GGC CGT CGC CTG T) and for successful integration of PvDBP PvW1 allele (ol186 fwd and ol1799 rev-TCC CGT TCT TCC CAT CTC CGG T).

Samples were analyzed by the GIA Assay Reference Center, Laboratory of Malaria and Vector Research, National Institute of Allergy and Infectious Diseases, National Institutes of Health. The GIA assay methodology has been published elsewhere (*38*). In brief, 10 mg/mL purified total IgG (Protein G purified from serum) were mixed with about 1.5 % of trophozoite-rich parasites in a final volume of 40 µL in 96-well plates. After about 27 h of incubation, the relative parasitemia in each well was determined by parasite lactate dehydrogenase (pLDH) activity. Test IgG samples which showed greater than 10% GIA in the first assay were tested in two more independent assays, and median % GIA values from the three assays are reported.

Flow cytometry T cell assay

Flow cytometry was performed using frozen aliquots of PBMC from donors on day 0 (pre-vaccination) and 14 days and 28 days post-final vaccination with either VV-DBPII or PvDBPII/M-M. Cryopreserved PBMC were thawed and rested at 37°C before an 18 h 37°C stimulation in the dark with medium alone, 2.5 µg/peptide/mL of a PvDBPII 20mer peptide pool (Mimotopes) (**table S5**), or 1 µg/mL Staphylococcal enterotoxin B (SEB; S-4881, Sigma; positive control). Anti-CD28 (1 µg/mL; 16-0289-85, eBioscience, clone: CD28.2), anti-CD49d (1 µg/mL; 16-0499-85, eBioscience, clone: 9F10) and anti-CD107a-phycoerytrhin (PE)-cyanine (Cy) 5 (1/2550 dilution; 15-1079-42, eBioscience, clone: eBioH4A3) were included in the cell culture medium. Brefeldin A (00-4506-51, eBioscience) and monensin (00-4505-51, eBioscience) were added after 2 h. Following incubation, PBMC were stained and fixed with Cytofix/Cytoperm (554714, BD Biosciences). The following anti-human antibody and dye were used (20 minutes, room temperature, in the dark) prior to fixation: anti-CCR7-brilliant violet (BV) 711 (1/50 dilution; 353228, clone: G043H7, BioLegend); and Live/Dead Aqua (1/20 dilution; L34966, Invitrogen). The following anti-human antibodies and dyes were used (30 minutes, room temperature, in the dark) after fixation: anti-CD14-eFluor 450 (1/200 dilution; 48-0149-42, clone: 61D3), anti-CD19-eFluor 450 (1/200 dilution; 48-0199-42, clone: HIB19), anti-CD8a-allophycocyanine (APC)-eFluor 780 (1/10 dilution; 47-0088-42, clone: RPA-T8), anti-interferon (IFN)-γ-fluorescein isothiocyanate (FITC) (1/500 dilution; 11-7319-82, clone: 4S.B3), anti-tumor necrosis factor (TNF)-α-PE-Cy7 (1/2000 dilution; 25-7349-82, clone: MAb11), anti-CD3-Alexa Fluor 700 (1/100 dilution; 56-0038-82, clone: UCHT1) – all eBioscience; anti-CD4-peridinin chlorophyll protein (PerCP)-Cy5.5 (1/14 dilution; 300530, clone: RPA-T4), anti-interleukin (IL)-2-BV650 (1/50 dilution; 500334, clone: MQ1-17H12), anti-IL5-PE (1/40 dilution; 500904, clone: JES-39D10), anti-IL-13-APC (1/20 dilution; 501907, clone: JES10-5A2), anti-CD45RA-BV605 (1/2000 dilution; 304134, clone: HI100) – all BioLegend. Samples were acquired on a Fortessa flow cytometer using BD FACSDiva (both BD Biosciences) and data were analyzed in FlowJo (v10.8, Treestar).

Blood-stage inoculum preparation and CHMI

The PvW1 blood-stage inoculum was thawed and prepared under strict aseptic conditions as previously described (*39*). The required number of vials of the cryopreserved stabilate (each containing approximately 0.5 mL of red blood cells in 1 mL of Glycerolyte 57) were thawed in parallel in an area using solutions licensed for clinical use and single-use disposable consumables. A class II microbiological safety cabinet (MSC) was used to prepare the inoculum, which was fumigated with hydrogen peroxide and decontamination validated prior to use. To prepare the inoculum, 0.2 volume 12 % saline was added dropwise to the contents (about 1.5 mL) of each vial of thawed

infected blood. Each sample was left for 5 min, before an additional 10 volumes of 1.6 % saline was added dropwise prior to centrifugation for 4 min at 830 x *g*. Each supernatant was removed and 10 mL of 0.9 % saline was added dropwise. The cell pellets were pooled and washed twice in 0.9 % saline before a final resuspension into one 10 mL sample in 0.9 % saline. This 10 mL suspension was then divided into aliquots, equivalent to one tenth of one original cryovial. Each aliquot was made up to a total volume of 5 mL in 0.9 % saline in a sterile syringe for injection and transported to the clinic. For each challenge, one dose of the 1:10 diluted inoculum was quantified by quantitative polymerase chain reaction (qPCR) to be equivalent to between 165 to 217 genome copies of *P. vivax*. This will be an overestimate of the number of live viable parasites administered per volunteer because some parasites will be killed during the inoculum thawing and preparation process.

The reconstituted blood-stage inoculum (5 mL per syringe) was injected intravenously using an indwelling cannula, preceded and followed by a saline flush. The inoculum was administered to all volunteers within a maximum of 3 h 7 min from thawing of the inoculum. Volunteers were observed for 1 h following injection of the inoculum before discharge from the clinical facility. Following each CHMI, a leftover sample of the inoculum was cultured and shown to be negative for bacterial contamination.

Malaria parasite quantification by qPCR

qPCR was used to measure *P. vivax* parasitemia in volunteers' blood in real-time as previously described (*39*) using an assay that targets the 18S ribosomal RNA (rRNA) gene. DNA was extracted from 0.4 mL whole EDTA blood using a QIAsymphony SP robot, utilizing the Qiagen DSP Blood Midi Kit and the pre-loaded Blood 400 v6 extraction protocol, with a 100 µL elution in ATE buffer selected. Additionally, aliquots of baseline samples taken within 2 days pre-CHMI were spiked with a known concentration of positive control DNA to check there was no presence of PCR inhibitors in volunteers' blood prior to CHMI.

Following DNA extraction, a standard Taqman absolute quantitation was used against a standard curve to amplify a 183 bp PCR product from the multi-copy, highly conserved 18S ribosomal RNA genes of *Plasmodium spp.* qPCR used the following adapted oligonucleotide primers and probe (*40*): 18s forward primer 5'-AGG AAG TTT AAG GCA ACA ACA GGT-3', 18s reverse primer 5'-GCA ATA ATC TAT CCC CAT CAC GA-3' and shortened FAM labelled probe sequence 5'-TGA ACT AGG CTG CAC GCG-3', was run on an ABI StepOne Plus machine with v2.3 software. Default Universal qPCR (target FAM-NFQ-MGB) and quality control (QC) settings were used apart from the use of 40 cycles and 25 µL reaction volume.

This qPCR detects DNA from pan-*Plasmodium* species, but unlike the synchronous growth of *P. falciparum*, circulating *P. vivax*-infected red blood cells may contain up to 10 to 15 individual genomes (in blood-stage late trophozoites and schizonts) and can also include the presence of gametocytes. The qPCR score is therefore reported in genome copies/mL (gc/mL) as opposed to a quantity of parasites.

The standard curve was generated from dilution of a linearized plasmid encoding part of the *Plasmodium spp.* 18S ribosomal RNA gene and calibrated using known *P. falciparum* (Pf) spiked blood samples initially and then reference DNA extracted from whole blood from *P. vivax*-infected patient samples in Thailand where parasites had been quantified by microscopy (kindly provided by Mahidol University). Based upon earlier results obtained using dilution series of microscopically-counted cultured Pf parasites, a Pf-specific 18S rRNA Taqman qPCR showed a lower limit of quantification (LLQ, defined as % covariance [CV] <20%) of around 20 Pf parasites (p)/mL blood(*41*). Counted parasite dilution series results also suggested that the lower limit of probable detection (LLD, that is a probability of >50% of ≥1 positive result among three replicate qPCR reactions) is in the region of 5 p/mL, whereas samples at 1 p/mL are consistently negative (24/24 qPCR reactions). Positive results in this assay (even at very low detection) are thus essentially 100 % specific for genuine parasitemia, with positive results beneath the LLQ likely to signify parasitemia in the range of 2 to 20 p/mL. Similar sensitivity in terms of genome copy detection was observed when using the pan-*Plasmodium* qPCR described above and the diluted *P. vivax*-infected patient blood test samples from Thailand. As noted, these samples had microscopically mixed life stages with varying copies of the 18S rRNA gene and thus the assay readout is reported in terms of gc/mL. Based on this and the above experiments, 20 gc/mL was set as the lower limit of detection to meet positive reporting criteria, but all raw data are shown in the Results.

For QC purposes, qPCR samples were re-tested if replicates included a mixture of positive and negative (in terms of amplification) results with one or more positive results > 100 gc/mL or if the % CV of any results were high outliers. All ‘passed’ data following the quality control steps above, including any 0 values, were used to generate the final mean qPCR result for each time-point.

Thick blood film microscopy

Collection of blood, preparation of thick films and slide reading were performed according to Jenner Institute Standard Operating Procedure (SOP) ML009. Slides were prepared using Field’s stain A and then Field’s stain B. 200 fields at high power (1000x) were read. Visualization of two or more parasites in 200 high power fields constituted a positive result. For internal quality control, all slides were read separately by two experienced microscopists, with a third read if results were discordant (one negative and one positive report).

Modelling of parasite multiplication rate

A qPCR-derived parasite multiplication rate (PMR) was modelled based on previously described methodology with modifications (*39, 41*). The arithmetic mean of three replicate qPCR results obtained for each individual at each time-point was used for model-fitting. Negative replicates and any qPCR data points below 20 gc/mL, based upon the mean of the three replicates, were removed prior to model-fitting. Data from timepoints in CHMIs conducted in September 2019 and May 2021, which would not have been available if using the visit schedule for the final CHMI in October 2021 (VAC069D /VAC071B /VAC079B), were also removed prior to model-fitting. The time interval between the morning and evening bleeds used for qPCR monitoring was set as 0.37 days. PMR per 48 h was then calculated using a linear model fitted to $\log_{10}$-transformed qPCR data.

Analysis of $\log_{10}$ cumulative parasitemia during CHMI

The arithmetic mean of three replicate qPCR results obtained for each individual at each time-point up until day C+14, when the first volunteer reached malaria diagnostic criteria across all CHMIs, was used for analysis. As per PMR modelling, negative replicates and any qPCR data points below 20 gc/mL, based upon the mean of the three replicates, were removed prior to analysis, as well as removal of data from timepoints in CHMIs conducted in September 2019 and May 2021, which would not have been available if using the visit schedule for the final CHMI in October 2021. Log_{10} cumulative parasitemia was then calculated from area under the curve analysis of $\log_{10}$-transformed qPCR data, where a peak was defined as any positive value above baseline.

Supplementary Figures

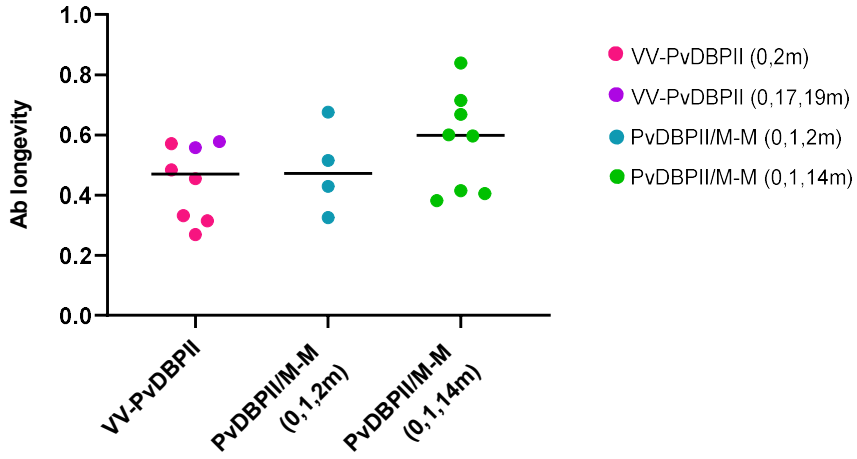

Figure S1. Antibody (Ab) longevity post-final vaccination.

For each individual, the area under the curve was calculated from the time of their peak anti-PvDBPII (SalI) total IgG response until the final timepoint available and divided by their peak antibody titer and duration over which the area under the curve was calculated in order to estimate the antibody longevity. Comparisons between groups with Kruskal-Wallis test were not statistically significant. m, month. Group medians are shown. Colored symbols indicate vaccination regimens.

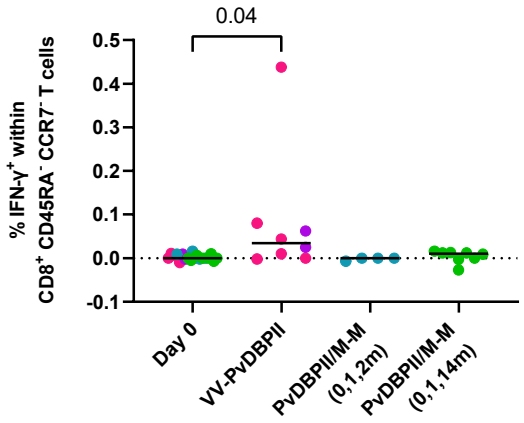

Figure S2. PvDBPII-specific CD8$^+$ T cell responses 14 days post-final vaccination.

Percentage of IFN-γ$^+$ cells within CD8$^+$ CD45RA$^-$ CCR7$^-$ effector memory T cells at 14 days post-final vaccination following PBMC stimulation with a pool of PvDBPII (SalI) peptides. The frequency of IFN-γ$^+$ cells in sample-matched unstimulated wells was subtracted to control for non-specific activation. Baseline responses (Day 0) are shown for all volunteers. *p* value as calculated by Kruskal-Wallis test with Dunn's multiple comparison post-test. Group medians are shown. Colored symbols indicate vaccination regimens as in fig. S1.

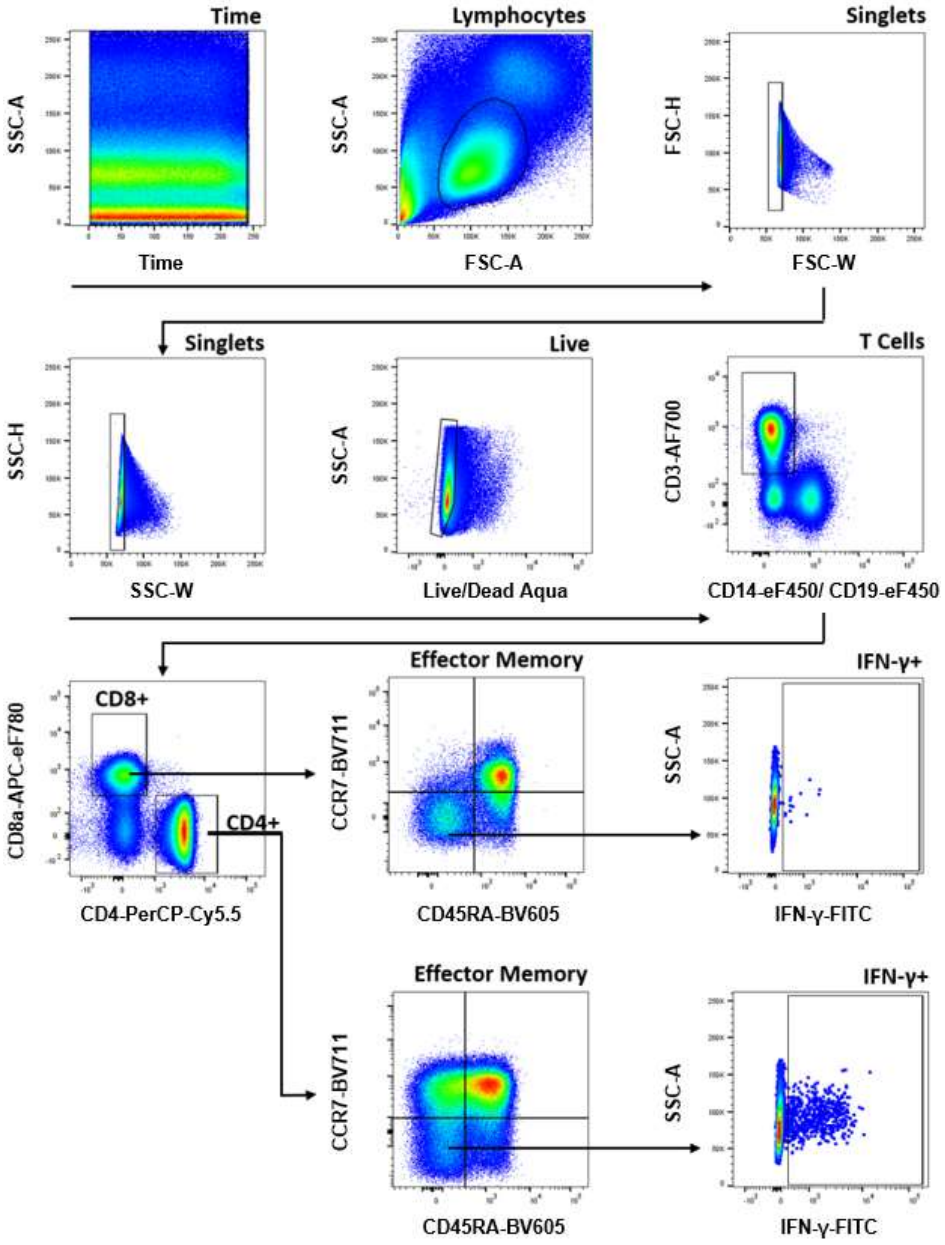

Figure S3. Flow cytometry gating strategy.

Gating strategy for definition of live singlet $CD4^+$ and $CD8^+$ effector memory T cells, and for gating of IFN-γ^+ cells within the live singlet $CD4^+$ and $CD8^+$ effector memory T cell populations. SSC, side scatter; FSC, forward scatter; A, area; H, height; W, width; eF, eFluor; AF, Alexa Fluor.

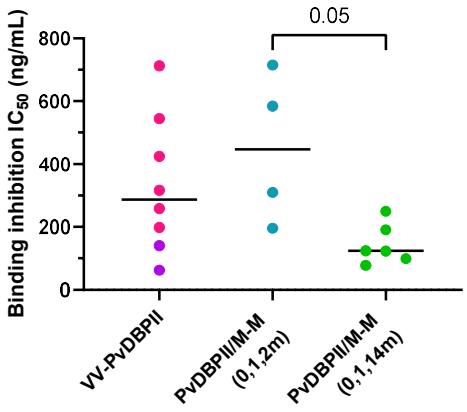

Figure S4. DARC-PvDBPII binding inhibition.

The concentration of anti–PvDBPII total IgG that is required to achieve 50% binding inhibition (IC_{50}) was calculated for each individual by dividing their serum anti-PvDBPII (SalI) total IgG concentration by the dilution factor of serum required to inhibit binding of DARC to PvDBPII (SalI) by 50%. Group medians are shown. *p* value as calculated by Kruskal-Wallis test with Dunn's multiple comparison post-test. Colored symbols indicate vaccination regimens as in fig. S1.

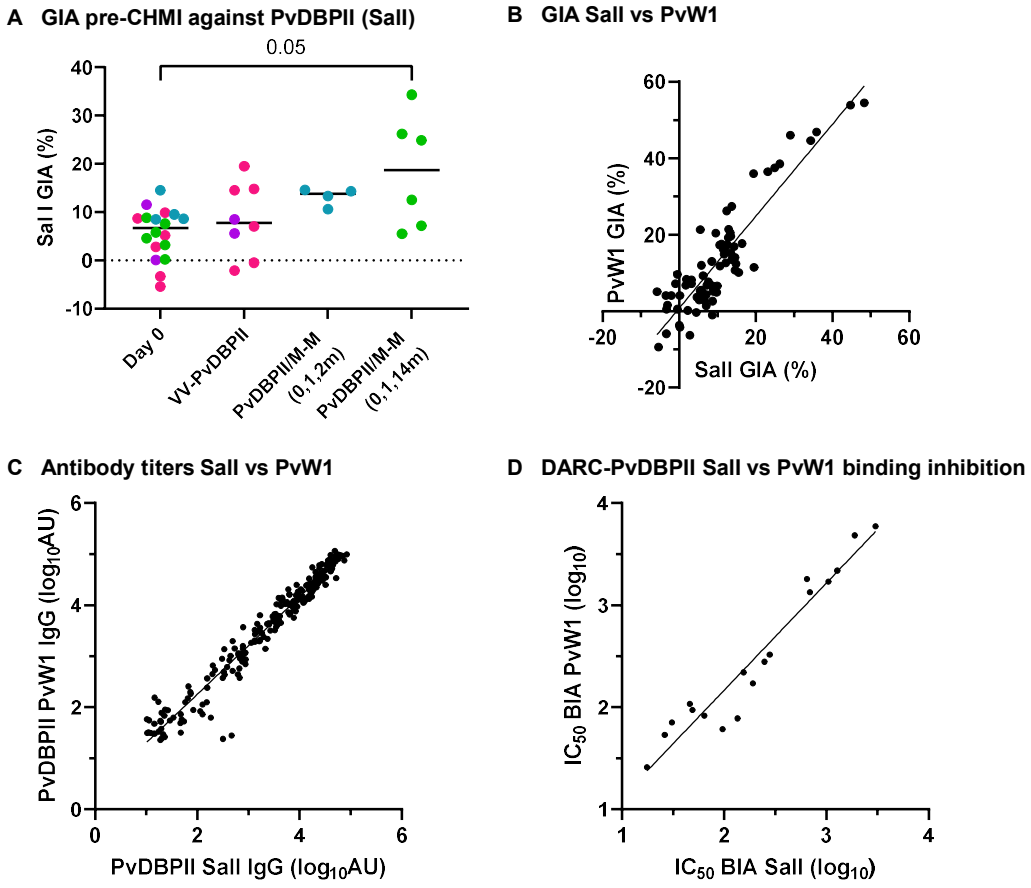

E

	Growth inhibition	Antibody titers	Binding inhibition
Slope	1.20	0.95	1.05
95% CI	1.07 to 1.34	0.93 to 0.98	0.90 to 1.20
R^2	0.81	0.95	0.93
n	75	230	18

Figure S5. Analysis of anti-PvDBPII SalI versus PvW1 GIA, ELISA and BIA responses.

(**A**) Percentage in vitro growth inhibition activity (GIA) of 10 mg/mL total IgG, taken pre-CHMI, against *P. knowlesi* expressing the PvDBP SalI allele. Baseline responses (Day 0) are shown for all volunteers. *p* values were calculated by Kruskal-Wallis test with Dunn's multiple comparison post-test. Horizontal lines indicate group medians. Colored symbols indicate vaccination regimens as in fig. S1. (**B**) Data from all volunteers and timepoints at which GIA of 10 mg/mL total IgG against both *P. knowlesi* expressing the PvDBP PvW1 allele and *P. knowlesi* expressing the PvDBP SalI allele are shown with linear regression line. (**C**) ELISA data from all volunteers and timepoints at which anti-PvDBPII total IgG responses against SalI and PvW1 alleles were assessed in serum. Responses to PvDBPII are reported in $\log_{10}$ arbitrary units (AU) with linear regression line. (**D**) Data from all volunteers and timepoints at which BIA in serum were assessed by inhibition of recombinant DARC-

PvDBPII binding against SalI and PvW1 alleles. Log_{10} dilution factors of individual serum required to inhibit binding of DARC to PvDBPII by 50% (IC_{50}) are reported with linear regression line. (**E**) Table summarizing parameters of linear regression of correlations shown in panels B, C and D. Slope, 95% confidence interval (CI) of slope, R squared and number of observations for each linear regression are shown.

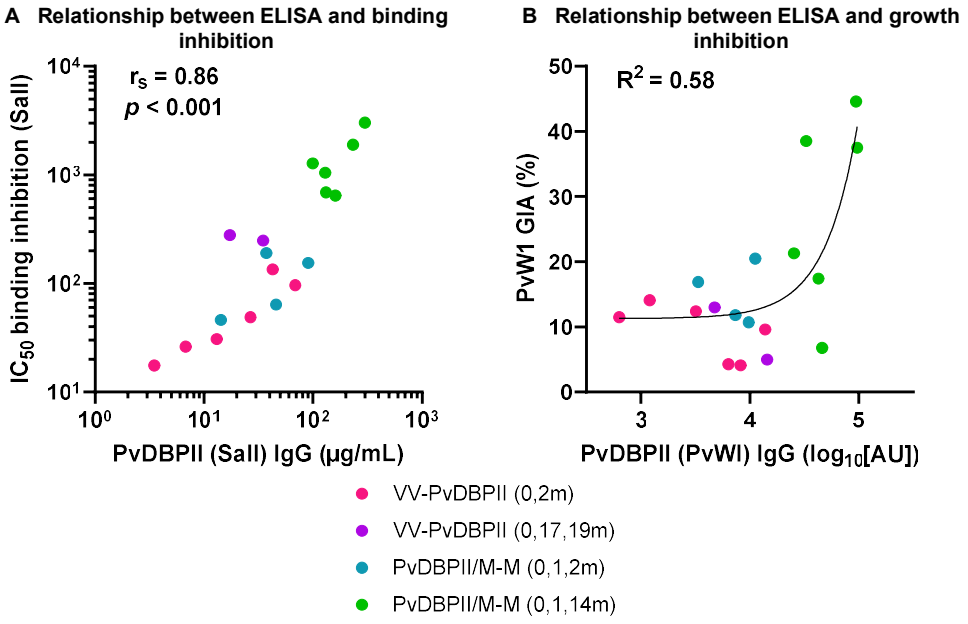

Figure S6. Relationships between measures of anti-PvDBPII antibody responses pre-CHMI.

(**A**) Correlation analysis between anti-PvDBPII (SalI) total IgG serum responses measured pre-CHMI by ELISA versus BIA measured at the same timepoint by IC_{50} values. Spearman's rank correlation coefficient and *p* value are shown, n=18. (**B**) Relationship between pre-CHMI *P. knowlesi* (PvW1) GIA assay data and anti-PvDBPII (PvWI) IgG response measured by ELISA in the purified serum IgG used in the assay. A non-linear regression curve is shown for all samples combined (solid line, n=18).

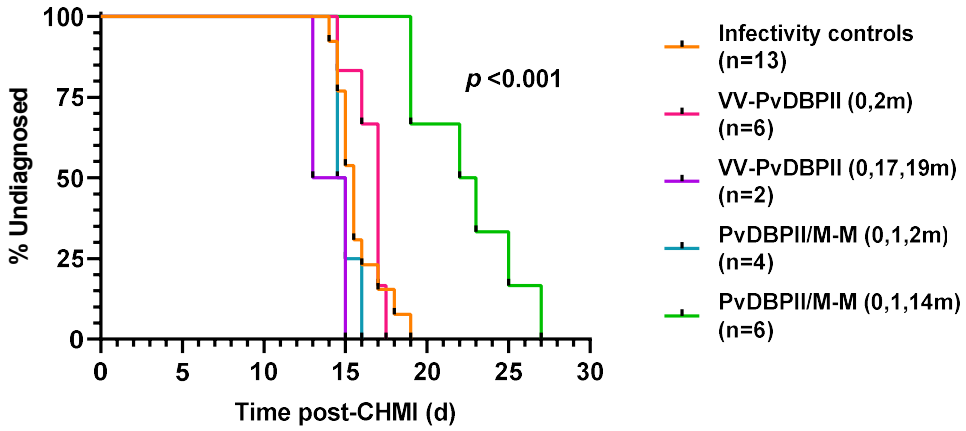

Figure S7. Kaplan-Meier plot of time to malaria diagnosis.

Median time to diagnosis was 15.5 days for controls and 22.5 days for PvDBPII/M-M delayed dosing regimen. Pairwise comparison with log-rank test between controls versus vaccine regimen groups was only significant for PvDBPII/M-M (0,1,14m) group (p <0.001).

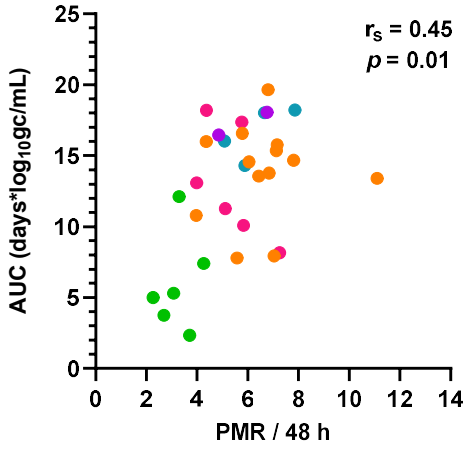

Figure S8. Relationship between in vivo parasite growth as measured by parasite multiplication rate versus $\log_{10}$ cumulative parasitemia.

Spearman's rank correlation coefficient and *p* value are shown, n=31. AUC, area under the curve. Colors indicate groups as in fig. S7.

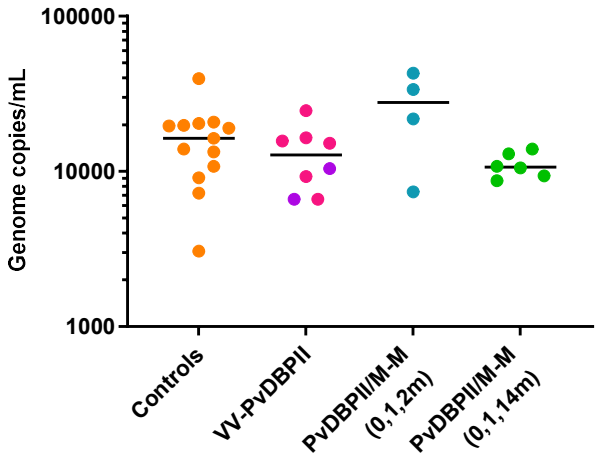

Figure S9. Malaria qPCR at diagnosis.

Parasitemia was measured by qPCR in gc/mL just prior to commencing anti-malarial treatment. Individual data and median values are shown. No significant differences were observed between the groups as measured by Kruskal-Wallis test with Dunn's multiple comparison post-test. Colors indicate groups as in fig. S7.

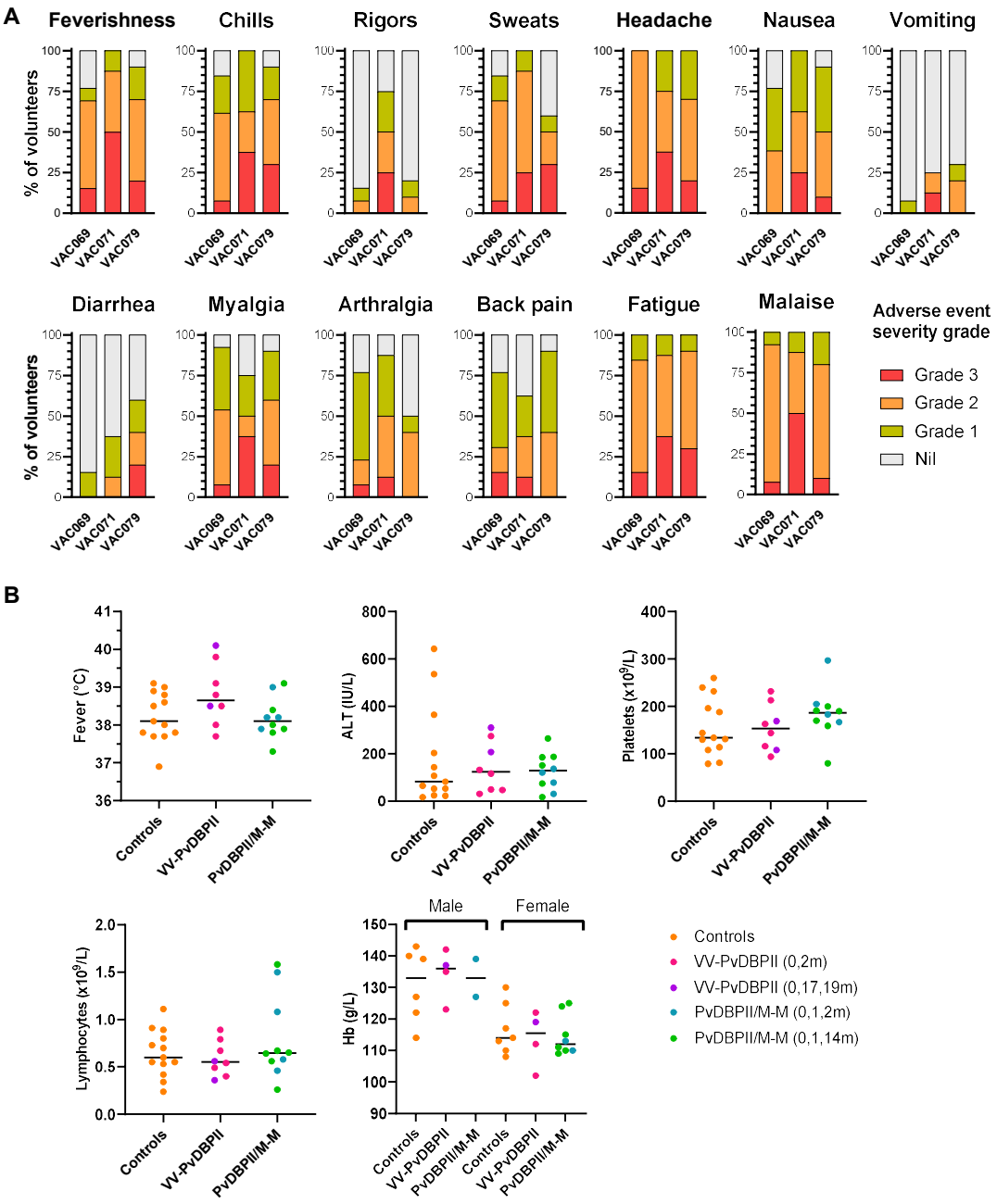

Figure S10. Clinical and laboratory adverse events during CHMI.

(**A**) Percentage of volunteers reporting solicited adverse events (AE) relating to malaria symptoms during CHMI. Maximum severity of each solicited AE reported by an individual is shown for control volunteers (VAC069, n=13), VV-PvDBPII vaccinees (VAC071, n=8) and PvDBPII/M-M vaccinees (VAC079, n=10). (**B**) Maximum recorded temperature, highest alanine transferase (ALT), lowest platelets, lowest lymphocytes and lowest hemoglobin (Hb) during CHMI is shown with medians. IU, international units. Horizontal lines represent medians.

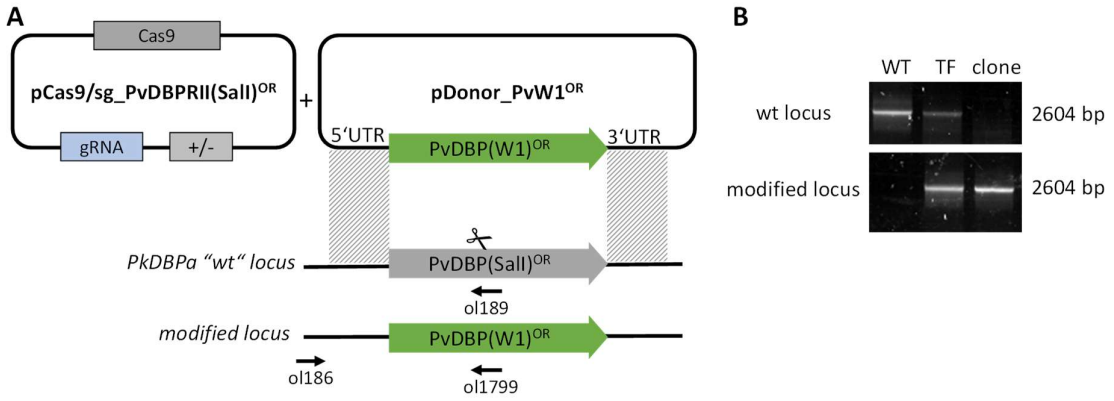

Figure S11. Design and genotypic analysis of *P. knowlesi* PvDBP PvW1 orthologue replacement line.

(**A**) Schematic detailing the approach to replace the coding sequence of PvDBP SalI allele with that of the PvDBP PvW1 allele within the previously generated transgenic *P. knowlesi* PvDBP^{OR}ΔβΔγ ("wild type", WT) strain. The pCas9/sg_PvDBPRII(SalI)^{OR} plasmid was transfected alongside the pDonor_PvW1^{OR}, to create a double strand break within the PvDBP SalI coding sequence and replace this with the PvDBP PvW1 allele by homologous recombination. Arrows indicate positions of diagnostic primers used for genotypic analysis of transfectants. (**B**) Parasites were analyzed by diagnostic PCR. Primer pairs were used to specifically detect wt locus (ol186 + ol189) and the modified locus (ol186 +ol1799) within i) the parental *P. knowlesi* PvDBP^{OR}ΔβΔγ (WT) strain; ii) bulk culture of transfectants (TF); and iii) a clonal transfectant (clone). The clonal *P. knowlesi* PvDBP^{OR} PvW1 transgenic parasite line was shown to only contain parasites with the PvW1 allele modified locus.

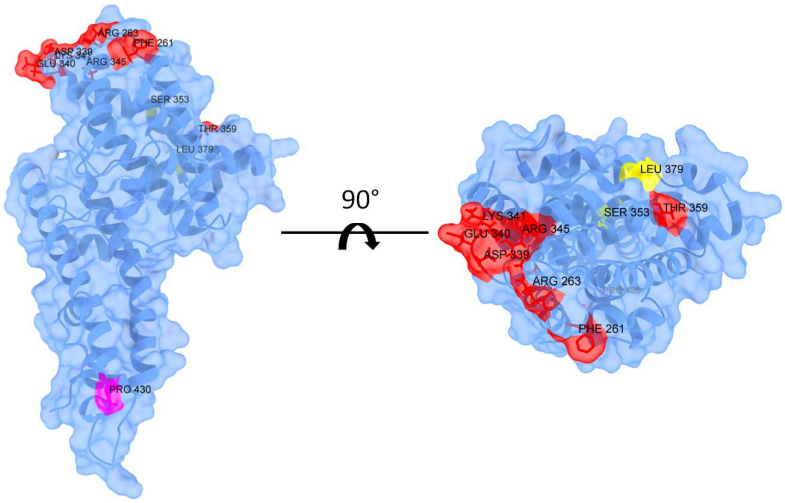

Amino acid position	261	263	339	340	341	345	353	359	379	430
PvW1	L	S	G	K	N	H	T	R	I	L
PvSalI	F	R	D	E	K	R	S	T	L	-

Figure S12. PvW1 polymorphisms mapped to the structure of PvDBPII SalI protein.

PvDBPII SalI strain (vaccine sequence) X-ray crystallography structure (PDB: 4NUU) annotated with sites of polymorphisms found in the PvWI strain (used for blood-stage CHMI) (*39*). Sites of non-conservative substitutions are shown in red, sites of conservative substitutions are shown in yellow, and sites of insertions are shown in pink. The table lists the amino acid polymorphisms within PvDBPII between SalI and PvW1 strains. The PvW1 sequence has a leucine insertion between positions 429 and 430 in the SalI sequence.

Supplementary Tables

Table S1. Baseline demographics of study participants. VV-PvDBPII indicates the viral-vectored vaccine; PvDBPII/M-M indicates the protein in Matrix-M adjuvant vaccine; CHMI indicates those volunteers who underwent controlled human malaria infection. *Samples from volunteers who were not heterozygous on Duffy blood group antigen (Fy) serophenotyping were also sent for Duffy blood group antigen genotyping. Only one volunteer (in the control group) with $Fya^{-}Fyb^{+}$ serophenotype had the Duffy blood group antigen genotype $FY*B/FY*B^{ES}$, whereby the erythrocyte silent (ES) allele has a mutation that prevents Fyb antigen expression in red blood cells.

		CHMI Controls	VV-PvDBPII		PvDBPII/M-M	
			All vaccinees	CHMI	All vaccinees	CHMI
No. of participants		13	16	8	16	10
Sex no.	Female	7	7	4	12	8
Age - median (range)		26 (21, 48)	25.5 (20, 44)	29 (21, 41)	28.5 (19, 44)	37 (21, 44)
Ethnicity no.	White	10	13	8	15	10
	Asian	1	2	0	0	0
	Arab	1	1	0	0	0
	Mixed	1	0	0	1	0
Duffy phenotype no.	$Fya^{+}Fyb^{-}$	3		2		1
	$Fya^{-}Fyb^{+}$	2*		4		3
	$Fya^{+}Fyb^{+}$	8		2		6

Table S2. Laboratory abnormalities following vaccinations. Number of episodes of laboratory abnormalities within 28 days following vaccinations with chimpanzee adenovirus 63 (ChAd63) PvDBPII, modified vaccinia virus Ankara (MVA) PvDBPII, or PvDBPII/Matrix-M. Maximal grade of laboratory abnormality, deemed at least possibly related to vaccination, is reported. V1 indicates first vaccination, V2 indicates second vaccination, and V3 indicates third vaccination.

Laboratory abnormality	Number of episodes					
	ChAd63 PvDBPII		MVA PvDBPII	PvDBPII/M-M		
	V1 (n=16)	V2 (n=2)	V1 (n=8)	V1 (n=16)	V2 (n=15)	V3 (n=12)
Leukopenia						
Grade 1	2	0	0	0	0	0
Lymphopenia						
Grade 1	5	1	0	0	4	2
Grade 2	6	0	2	1	1	2
Neutropenia						
Grade 1	3	0	0	0	0	1
Grade 2	2	0	0	0	0	0
Eosinophilia						
Grade 1	1	0	0	0	0	0
Hypokalemia						
Grade 1	3	1	0	0	0	0
Grade 3	0	1	0	0	0	0
Hyperbilirubinemia						
Grade 1	1	0	0	0	0	0
Anemia						
Grade 1	0	0	0	0	0	1
Thrombocytopenia						
Grade 1	0	0	0	1	0	0

Table S3. Unsolicited adverse events (AE) following ChAd63 or MVA PvDBPII vaccination. Unsolicited AEs occurring within 28 days of vaccination and deemed at least possibly related to ChAd63 or MVA PvDBPII vaccination. Number of episodes of unsolicited AE are listed by vaccine and MEDDRA System Organ Class and Preferred Term. Unsolicited AEs were of maximal grade 2 severity.

Unsolicited AE	Number of episodes of AE	
	ChAd63 PvDBPII	MVA PvDBPII
Gastrointestinal disorders		
Diarrhea	1	0
Abdominal pain upper	1	0
Vomiting	1	0
Dry mouth	1	0
Respiratory, thoracic and mediastinal disorders		
Rhinitis	1	1
Oropharyngeal pain	1	1
Cough	0	1
Skin and subcutaneous tissue disorders		
Rash	1	0
Musculoskeletal and connective tissue disorders		
Neck pain	1	0
Pain in extremity	1	0
Reproductive system and breast disorders		
Dysmenorrhea	2	0
Eye disorders		
Dry eye	1	0
General disorders and administration site conditions		
Chest pain	1	0
Nervous system disorders		
Paresthesia	0	1
Metabolism and nutrition disorders		
Decreased appetite	0	1

Table S4. Unsolicited AEs following PvDBPII/M-M vaccination. Unsolicited AEs occurring within 28 days of vaccination and deemed at least possibly related to PvDBPII/M-M vaccination. Number of episodes of unsolicited AE following the first, second, and third vaccination are listed by MEDDRA System Organ Class and Preferred Term. Unsolicited AEs were of maximal grade 2 severity.

Unsolicited AE	Number of episodes of AE with PvDBPII/M-M			
	V1 (n=16)	V2 (n=15)	V3 (n=12)	Total
Gastrointestinal disorders				
Diarrhea	0	1	0	1
General disorders and administration site conditions				
Administration site induration	1	0	0	1
Chest discomfort	1	0	0	1
Injection site pruritus	2	0	0	2
Injection site swelling	1	0	0	1
Swelling	1	0	0	1
Infections and infestations				
Rhinitis	1	0	0	1
Musculoskeletal and connective tissue disorders				
Back pain	2	1	0	3
Pain in extremity	2	1	0	3
Nervous system disorders				
Dizziness	1	0	0	1
Headache	0	2	1	3
Migraine	1	0	0	1
Hypoesthesia	0	1	0	1
Paresthesia	2	0	0	2
Somnolence	0	1	0	1
Taste disorder	1	0	0	1
Psychiatric disorders				
Euphoric mood	1	0	0	1
Insomnia	1	1	1	3
Tearfulness	1	0	0	1
Reproductive system and breast disorders				
Dysmenorrhea	0	1	0	1
Respiratory, thoracic and mediastinal disorders				
Nasal congestion	1	0	0	1
Oropharyngeal pain	0	1	0	1

Throat irritation	1	1	0	2

Table S5. PvDBPII peptides used for T cell stimulation. The PvDBPII SalI amino acid sequence was used to design 20mer peptides overlapping by 12 amino acids and these were synthesized by Mimotopes. Each stock was reconstituted to 50 mg/mL in dimethyl sulfoxide. A 200 µg/peptide/mL working stock of PvDBPII peptides was prepared by adding an equal amount of each peptide to cell culture medium for a final total peptide concentration of 8 mg/mL.

Peptide Number	N-terminus	Amino Acid Sequence	C-terminus
1	H-	DHKKTISSAIINHAFLQNTVGSG(261)	-NH2
2	Biotin-	SGSGAIINHAFLQNTVMKNCNYKR	-NH2
3	Biotin-	SGSGQNTVMKNCNYKRKRRERDWD	-NH2
4	Biotin-	SGSGNYKRKRRERDWDCNTKKDVC	-NH2
5	Biotin-	SGSGRDWDCNTKKDVCIPDRRYQL	-NH2
6	Biotin-	SGSGKDVCIPDRRYQLCMKELTNL	-NH2
7	Biotin-	SGSGRYQLCMKELTNLVNNTDTNF	-NH2
8	Biotin-	SGSGLTNLVNNTDTNFHRDITFRK	-NH2
9	Biotin-	SGSGDTNFHRDITFRKLYLKRKLI	-NH2
10	Biotin-	SGSGTFRKLYLKRKLIYDAAVEGD	-NH2
11	Biotin-	SGSGRKLIYDAAVEGDLLLKLNNY	-NH2
12	Biotin-	SGSGVEGDLLLKLNNYRYNKDFCK	-NH2
13	Biotin-	SGSGLNNYRYNKDFCKDIRWSLGD	-NH2
14	Biotin-	SGSGDFCKDIRWSLGDFGDIIMGT	-NH2
15	Biotin-	SGSGSLGDFGDIIMGTDMEGIGYS	-NH2
16	Biotin-	SGSGIMGTDMEGIGYSKVVENNLR	-NH2
17	Biotin-	SGSGIGYSKVVENNLRSIFGTDEK	-NH2
18	Biotin-	SGSGNNLRSIFGTDEKAQQRRKQW	-NH2
19	Biotin-	SGSGTDEKAQQRRKQWWNESKAQI	-NH2
20	Biotin-	SGSGRKQWWNESKAQIWTAMMYSV	-NH2
21	Biotin-	SGSGKAQIWTAMMYSVKKRLKGNF	-NH2
22	Biotin-	SGSGMYSVKKRLKGNFIWICKLNV	-NH2
23	Biotin-	SGSGKGNFIWICKLNVAVNIEPQI	-NH2
24	Biotin-	SGSGKLNVAVNIEPQIYRWIREWG	-NH2
25	Biotin-	SGSGEPQIYRWIREWGRDYVSELP	-NH2
26	Biotin-	SGSGREWGRDYVSELPTEVQKLKE	-NH2
27	Biotin-	SGSGSELPTEVQKLKEKCDGKINY	-NH2
28	Biotin-	SGSGKLKEKCDGKINYTDKKVCKV	-NH2
29	Biotin-	SGSGKINYTDKKVCKVPPCQNACK	-NH2
30	Biotin-	SGSGVCKVPPCQNACKSYDQWITR	-NH2
31	Biotin-	SGSGNACKSYDQWITRKKNQWDVL	-NH2

32	Biotin-	SGSGWITRKKNQWDVLSNKFISVK	-NH2
33	Biotin-	SGSGWDVLSNKFISVKNAEKVQTA	-NH2
34	Biotin-	SGSGISVKNAEKVQTAGIVTPYDI	-NH2
35	Biotin-	SGSGVQTAGIVTPYDILKQELDEF	-NH2
36	Biotin-	SGSGPYDILKQELDEFNEVAFENE	-NH2
37	Biotin-	SGSGLDEFNEVAFENEINKRDGAY	-NH2
38	Biotin-	SGSGFENEINKRDGAYIELCVCSV	-NH2
39	Biotin-	SGSGDGAYIELCVCSVEEAKKNTQ	-NH2
40	Biotin-	SGSGIELCVCSVEEAKKNTQEVVT	-OH

Table S6. Malaria qPCR data (gc/mL) for CHMI in September 2019. Malaria qPCR data used in PMR modelling are shown. The top row represents day (D) of follow-up visit post blood-stage CHMI. DoD indicates the timepoint at which malaria diagnostic criteria were reached. VAC069 Group 6, infectivity controls; VAC071 Group 1, VV-PvDBPII given at 0, 2 months. Treatment in some volunteers was started half a day after reaching malaria diagnostic criteria. qPCR data shown for samples taken prior to starting treatment. qPCR negative values for all three triplicate readings in the assay are indicated by 'N'. Squares highlighted in gray indicate negative or < 20 gc/mL which is below minimum positive reporting criteria and these datapoints were removed for PMR modelling. Datapoints which would not have been taken during CHMI in October 2021 due to changes in protocol were removed for PMR modelling and are not shown. Blacked out boxes indicate the timepoints after a volunteer commenced antimalarial treatment.

Trial	Group	DoD	D7	D8	D9	D10	D11	D11.5	D12	D12.5	D13	D13.5	D14	D14.5	D15	D15.5	D16	D16.5	D17	D17.5
VAC069	6	15.5	N	N	45	104	209		270		1379	1391	2244	3670	8921	9574	16345			
VAC069	6	14.5	N	9	72	N	265		778		3365	2835	4283	17392	19589					
VAC071	1	17	11	9	N	16	54		198		608		792		3098	3281	3694	4831	16135	15663
VAC071	1	17	N	N	26	13	80		94		362		652		2768	2751	4192	3832	15176	
VAC071	1	17.5	N	27	31	44	74		123		527		1285	889	2745	2295	2465	2914	9588	9263

Table S7. Malaria qPCR data (gc/mL) for CHMI in May 2021. Malaria qPCR data used in PMR modelling are shown. Top row represents day (D) of follow-up visit post blood-stage CHMI. DoD indicates the timepoint at which malaria diagnostic criteria were reached. VAC069 Group 9, infectivity controls; VAC079 Group 1, PvDBPII/M-M given at 0, 1, 14 months. Treatment in some volunteers was started half a day after reaching malaria diagnostic criteria. qPCR data shown for samples taken prior to starting treatment. qPCR negative values for all three triplicate readings in the assay are indicated by 'N'. Squares highlighted in gray indicate negative or < 20 gc/mL which is below minimum positive reporting criteria and these datapoints were removed for PMR modelling. Datapoints which would not have been taken during CHMI in October 2021 due to changes in protocol were removed for PMR modelling and are not shown. Blacked out boxes indicate the timepoints after a volunteer commenced antimalarial treatment.

Trial	Group	DoD	D7	D8	D9	D10	D11	D11.5	D12	D12.5	D13	D13.5	D14	D14.5	D15	D15.5	D16	D16.5	D17	D17.5	D18
VAC069	9	15.5	N	N	74	220	316		408		1678	1315	3625	6183	8674	9095					
VAC069	9	18	10	N	8	N	125		88		291		814	1252	1652	1805	2152	6550	7261	6161	12050
VAC069	9	19	N	N	26	37	98		62		268		298		1111	1262	1617	2121	6005	6395	4758
VAC069	9	14	32	35	108	182	1059	748	1121	2572	8025	7805	14766	18983							
VAC069	9	16	11	N	47	74	311		298		1669	1544	3316	6509	8709	9292	15568	39496			
VAC069	9	14.5	N	N	50	96	370		754		2641	2335	4847	12160	7238						
VAC069	9	15	N	N	113	183	485		556		3001	2476	5926	7904	16068	20776					
VAC079	1	19	6	21	17	31	79		73		316		379		798		1038	1474	3570	3555	3665
VAC079	1	19	N	N	18	15	77		135		155		442		719		1101	1578	3775	3861	2797
VAC079	1	25	N	N	N	15	6		25		34		52		70		166		429		306
VAC079	1	22	N	N	N	N	5		18		23		100		60		243		568		793
VAC079	1	27	1	N	N	N	27		23		34		28		27		107		49		57
VAC079	1	23	N	N	7	N	27		6		40		40		151		194		370		494

Trial	Group	DoD	D18.5	D19	D19.5	D20	D20.5	D21	D21.5	D22	D22.5	D23	D23.5	D24	D24.5	D25	D25.5	D26	D26.5	D27	D27.5
VAC069	9	15.5																			

VAC069	9	18	**20348**																		
VAC069	9	19	**9432**	**19781**																	
VAC069	9	14																			
VAC069	9	16																			
VAC069	9	14.5																			
VAC069	9	15																			
VAC079	1	19	**3769**	**13066**	**10752**																
VAC079	1	19	**6564**	**12971**																	
VAC079	1	25		**968**		**745**		**2043**	**2019**	**3302**	**2464**	**4198**	**4425**	**6010**	**5591**	**15486**	**10533**				
VAC079	1	22		**2504**	**2008**	**3138**	**3749**	**8451**	**7364**	**12330**	**9359**										
VAC079	1	27		**86**		**173**		**397**		**565**		**930**		**1597**		**3766**	**3290**	**5621**	**5404**	**12220**	**8699**
VAC079	1	23		**1242**		**1338**		**3417**		**4662**	**7714**	**13665**	**13903**								

Table S8. Malaria qPCR data (gc/mL) for CHMI in October 2021. Malaria qPCR data used in PMR modelling. Top row represents day (D) of follow-up visit post blood-stage CHMI. DoD indicates the timepoint at which malaria diagnostic criteria was reached. VAC069 Group 12, infectivity controls; VAC071 Group 2, VV-PvDBPII given at 0, 17, 19 months; VAC079 Group 2, PvDBPII/M-M given at 0, 1, 2 months. Treatment in some volunteers was started half a day after reaching malaria diagnostic criteria. qPCR data shown for samples taken prior to starting treatment. qPCR negative values for all three triplicate readings in the assay are indicated by 'N'. Squares highlighted in gray indicate negative or < 20 gc/mL which is below minimum positive reporting criteria and these datapoints were removed for PMR modelling. Blacked out boxes indicate the timepoints after a volunteer commenced antimalarial treatment.

Trial	Group	DoD	D7	D8	D9	D10	D11	D11.5	D12	D12.5	D13	D13.5	D14	D14.5	D15	D15.5	D16	D16.5	D17	D17.5
VAC069	12	15	8	28	66	124	604		806		2823	2487	3759	3551	14373	10759				
VAC069	12	15	17	17	71	119	1021	804	1617	1727	3405	4145	5742	6828	17155	13910				
VAC069	12	17	N	9	N	7	73		46		510		501		1735	1792	3600	4258	12302	13366
VAC069	12	15.5	N	61	53	73	401		767		1552	1096	2597	2245	5737	3057				
VAC071	2	13	47	54	128	279	1252	1196	2498	2221	9116	10400								
VAC071	2	15	N	28	81	162	447		950		1941	1523	2321	1996	6614					
VAC071	3	16	27	60	73	107	620		912		1918	2059	2644	6468	7675	4376	12306	24606		
VAC071	3	14.5	N	70	76	219	517		885		3010	3061	5275	6615						
VAC071	3	17	9	N	17	39	123		102		400		787		2660	1875	4213	5979	15424	16420
VAC079	2	14.5	17	20	169	242	1227	989	1517	2934	5399	6277	8780	17594	33726					
VAC079	2	14.5	N	107	129	90	1244	852	1657	1751	2228	5138	8719	11292	42914					
VAC079	2	15	9	14	61	46	536		652		1961	2072	2070	1030	10301	7374				
VAC079	2	16	8	21	130	65	503		611		1855	1765	2681	4131	7432	5408	13620	21801		

Table S9. Summary of PMR analysis. *Two tailed *p* value reported for Mann-Whitney test comparing controls with each vaccine group.

	Controls	VV-PvDBPII	PvDBPII/M-M (0,1,2m)	PvDBPII/M-M (0,1,14m)
No of volunteers	13	8	4	6
Median PMR per 48 h	6.8	5.4	6.3	3.2
Range PMR per 48 h	4.0 to 11.1	4.0 to 7.3	5.1 to 7.9	2.3 to 4.3
D'Agostino & Pearson K^2 test	$p = 0.02$	$p = 0.78$	$p = 0.57$	
Mann-Whitney test*		$p = 0.14$	$p = 0.01$	

Table S10. Analysis of PMR by study group and Duffy blood group serophenotype. Multiple linear regression was used to test if PMR differed significantly between different Duffy blood group antigen (DARC) serophenotypes after controlling for vaccination group.

	Univariate predictor			Adjusted for other variable		
Variable	Estimate	95% CI	*p* value	Estimate	95% CI	*p* value
Intercept	6.6	5.8 to 7.4	<0.001	6.3	5.5 to 7.2	<0.001
Study group						
Controls	0			0		
VV-PvDBPII	-1.1	-2.4 to 0.2	0.08	-1.2	-2.5 to 0.2	0.08
PvDBPII/M-M (0,1,2m)	-0.2	-1.9 to 1.4	0.76	0.04	-1.6 to 1.7	0.96
PvDBPII/M-M (0,1,14m)	-3.4	-4.8 to -2.0	<0.001	-3.3	-4.7 to -1.9	<0.001
DARC serophenotype						
$Fya^{+}Fyb^{+}$				0		
$Fya^{+}Fyb^{-}$				1.2	-0.1 to 2.6	0.08
$Fya^{-}Fyb^{+}$				0.02	-1.2 to 1.3	0.97
R squared	0.49			0.56		
No observations	31			31		